



University of Kentucky  
UKnowledge

Chemistry Faculty Publications

Chemistry

3-30-2017

# Collective Quadrupole Behavior in $^{106}\text{Pd}$

Francisco M. Prados-Estévez

*University of Kentucky*, [francisco.prados-estevez@uky.edu](mailto:francisco.prados-estevez@uky.edu)

Erin E. Peters

*University of Kentucky*, [fe.peters@uky.edu](mailto:fe.peters@uky.edu)

A. Chakraborty

*Siksha Bhavana, India*

M. G. Mynk

*University of Kentucky*

D. Bandyopadhyay

*University of Kentucky*

*See next page for additional authors*

**Right click to open a feedback form in a new tab to let us know how this document benefits you.**

Follow this and additional works at: [https://uknowledge.uky.edu/chemistry\\_facpub](https://uknowledge.uky.edu/chemistry_facpub)



Part of the [Chemistry Commons](#), and the [Nuclear Commons](#)

---

## Repository Citation

Prados-Estévez, Francisco M.; Peters, Erin E.; Chakraborty, A.; Mynk, M. G.; Bandyopadhyay, D.; Boukharouba, N.; Choudry, S. N.; Crider, Benjamin P.; Garrett, P. E.; Hicks, S. F.; Kumar, A.; Lesher, S. R.; McKay, C. J.; McEllistrem, Marcus T.; Mukhopadhyay, Sharmistha; Orce, J. N.; Scheck, M.; Vanhoy, J. R.; Wood, J. L.; and Yates, Steven W., "Collective Quadrupole Behavior in  $^{106}\text{Pd}$ " (2017). *Chemistry Faculty Publications*. 106.  
[https://uknowledge.uky.edu/chemistry\\_facpub/106](https://uknowledge.uky.edu/chemistry_facpub/106)

---

**Authors**

Francisco M. Prados-Estévez, Erin E. Peters, A. Chakraborty, M. G. Mynk, D. Bandyopadhyay, N. Boukharouba, S. N. Choudry, Benjamin P. Crider, P. E. Garrett, S. F. Hicks, A. Kumar, S. R. Lesher, C. J. Mckay, Marcus T. McEllistrem, Sharmistha Mukhopadhyay, J. N. Orce, M. Scheck, J. R. Vanhoy, J. L. Wood, and Steven W. Yates

**Collective Quadrupole Behavior in  $^{106}\text{Pd}$** **Notes/Citation Information**

Published in *Physical Review C*, v. 95, issue 3, 034328, p. 1-18.

©2017 American Physical Society

The copyright holder has granted permission for posting the article here.

**Digital Object Identifier (DOI)**

<https://doi.org/10.1103/PhysRevC.95.034328>

# Collective quadrupole behavior in $^{106}\text{Pd}$

F. M. Prados-Estévez,<sup>1,2</sup> E. E. Peters,<sup>1</sup> A. Chakraborty,<sup>1,2,\*</sup> M. G. Mynk,<sup>1</sup> D. Bandyopadhyay,<sup>2</sup> N. Boukharouba,<sup>2</sup> S. N. Choudry,<sup>2</sup> B. P. Crider,<sup>2,†</sup> P. E. Garrett,<sup>3</sup> S. F. Hicks,<sup>4</sup> A. Kumar,<sup>2,‡</sup> S. R. Lesher,<sup>2,§</sup> C. J. McKay,<sup>2</sup> M. T. McEllistrem,<sup>2</sup> S. Mukhopadhyay,<sup>1,2</sup> J. N. Orce,<sup>2,||</sup> M. Scheck,<sup>2,¶</sup> J. R. Vanhoy,<sup>5</sup> J. L. Wood,<sup>6</sup> and S. W. Yates<sup>1,2</sup>

<sup>1</sup>Department of Chemistry, University of Kentucky, Lexington, Kentucky 40506-0055, USA

<sup>2</sup>Department of Physics & Astronomy, University of Kentucky, Lexington, Kentucky 40506-0055, USA

<sup>3</sup>Department of Physics, University of Guelph, Guelph, Ontario, N1G2W1, Canada

<sup>4</sup>Department of Physics, University of Dallas, Irving, Texas 75062, USA

<sup>5</sup>Department of Physics, United States Naval Academy, Annapolis, Maryland 21402, USA

<sup>6</sup>School of Physics, Georgia Institute of Technology, Atlanta, Georgia 30332, USA

(Received 19 December 2016; published 30 March 2017)

Excited states in  $^{106}\text{Pd}$  were studied with the  $(n, n'\gamma)$  reaction, and comprehensive information for excitations with spin  $\leqslant 6\hbar$  was obtained. The data include level lifetimes in the femtosecond regime, spins and parities, transition multipolarities, and multipole mixing ratios, which allow the determination of reduced transition probabilities. The  $E2$  decay strength to the low-lying states is mapped up to  $\approx 2.4$  MeV in excitation energy. The structures associated with quadrupole collectivity are elucidated and organized into bands.

DOI: [10.1103/PhysRevC.95.034328](https://doi.org/10.1103/PhysRevC.95.034328)

## I. INTRODUCTION

The structural interpretation of nuclei between spherical (closed-shell) and deformed (open-shell) regions, often called “transitional,” has been strongly influenced by the Bohr model [1], i.e., a “liquid-drop” model with quantized shape degrees of freedom. Thus, nuclei near closed shells are viewed as spherical, exhibiting harmonic quadrupole, octupole, etc. shape vibrations, and nuclei away from shell closures are interpreted as having static deformed quadrupole, etc. shapes with rotational and vibrational degrees of freedom.

For many years, the  $^{48}\text{Cd}$  isotopes were regarded as “textbook” cases of harmonic quadrupole vibrational behavior, based on patterns of excitation energies and  $\gamma$ -ray decay branching ratios. However, in a systematic study of stable even-mass Cd isotopes, it was concluded that some of these nuclei are poorly described by collective vibrational models [2–4]. This view arose following measurements of the detailed properties of excited states [5–7], including lifetimes, and left open the question of whether the neighboring  $^{46}\text{Pd}$  isotopes may exhibit near-harmonic quadrupole vibrational behavior as excitation energy patterns suggest.

In a Coulomb excitation study of  $^{106,108}\text{Pd}$ , Svensson and co-workers [8] concluded that vibrational degrees of freedom are important for the description of the low-spin level structure of these nuclei but that not all of the observed decay properties can be understood without invoking rotational motion and triaxiality. In  $g$ -factor measurements of the  $2_1^+$ ,  $2_2^+$ , and  $4_1^+$  states of  $^{106}\text{Pd}$ , Gündal *et al.* [9] examined the vibrational character of this nucleus and concluded that the excitation energies and  $g$  factors are consistent with the simple vibrational model, but the nonzero static quadrupole moment of the first excited state cannot be explained. The recent report of  $E0$  transitions in  $^{106}\text{Pd}$  with large  $\rho^2(E0)$  values provides evidence for shape coexistence and rotational bands are clearly evident [10].

In the present work, we carried out a detailed characterization of levels in  $^{106}\text{Pd}$  with the  $(n, n'\gamma)$  reaction to assess the conflicting pictures of the structure of nuclei in this mass region. These data provide a comprehensive view of the positive-parity structure up to  $\approx 2.4$  MeV for spins  $J \leqslant 6$ , as provided by  $E2$  transition strengths via lifetime measurements from Doppler shifts following inelastic neutron scattering. When combined with results from multistep Coulomb excitation [8,11], these data, i.e., spins, transition multipolarities, multipole mixing ratios, and decay branching ratios, provide a detailed view of the quadrupole collectivity of the low-spin states.

## II. EXPERIMENTS

The present study of the low-lying structure of  $^{106}\text{Pd}$  was performed via  $\gamma$ -ray spectroscopy following inelastic neutron scattering (INS). These measurements, executed at the University of Kentucky Accelerator Laboratory (UKAL), provide a detailed characterization of the low-lying excited states, including excitation energies, spins, parities, decay intensities, transition multipolarities, multipole mixing ratios, and level lifetimes. The nearly monoenergetic neutrons

\*Present Address: Department of Physics, Siksha Bhavana, Visva-Bharati, Santiniketan 731 235, West Bengal, India.

†Present Address: National Superconducting Cyclotron Laboratory (NSCL), Michigan State University, East Lansing, Michigan 48824, USA.

‡Present Address: Department of Physics, Panjab University, Chandigarh 1600014, India.

§Present Address: Department of Physics, University of Wisconsin-La Crosse, La Crosse, Wisconsin 54601-3742, USA.

||Department of Physics, University of the Western Cape, P/BX17, ZA-7535, South Africa.

¶School of Engineering and Computing, University of the West of Scotland, High Street, Paisley PA1 2BE, UK; SUPA, Scottish Universities Physics Alliance, Glasgow G12 8QQ, UK.

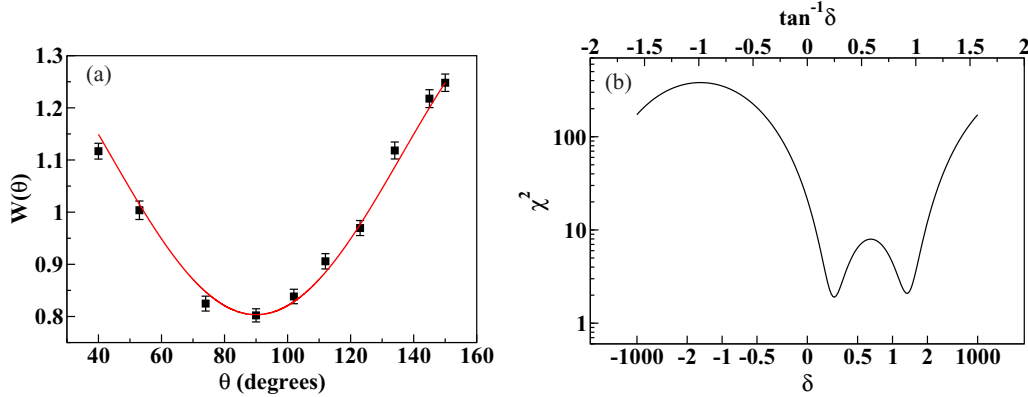


FIG. 1. (a) Angular distribution of the 1397.6 keV  $\gamma$  ray from the 1909.5 keV level measured at  $E_n = 2.2$  MeV and (b) plot of  $\chi^2$  vs mixing ratio,  $\delta$ , for the fit of the angular distribution in panel (a) with statistical model calculations.

( $\Delta E \approx 60$  keV at 2 MeV neutron energy) were provided through the  ${}^3\text{H}(p,n){}^3\text{He}$  reaction at the 7 MV Van de Graaff accelerator of the UKAL. The scattering sample consisted of 19.98 g of  ${}^{106}\text{Pd}$  metal powder, 98.53% enriched, in a cylindrical polyethylene container 1.8 cm in diameter and 3.5 cm in height. This sample was suspended at a distance of 5 cm from the end of a tritium gas cell used for neutron production. The  $\gamma$  rays from the  $(n,n'\gamma)$  reaction were detected with a high-purity germanium (HPGe) detector with a relative efficiency of 55% and an energy resolution of 2.1 keV full width at half maximum (FWHM) at 1332 keV. For the  $\gamma$ -ray singles measurements [12], an annular bismuth germanate (BGO) detector served for Compton suppression and as an active shield. The HPGe detector was 115 cm from the scattering sample. Both detectors were shielded by boron-loaded polyethylene, copper, and tungsten. Additional time-of-flight gating was employed to suppress background radiation and improve the peak-to-background ratio. The neutron flux was monitored with a  $\text{BF}_3$  long counter at  $90^\circ$  relative to the beam line and 3.78 m from the gas cell as well as by observing the time-of-flight spectrum of neutrons in a fast liquid scintillator (NE218) at an angle of  $43^\circ$  with respect to the beam axis and 5.9 m from the gas cell. Spectra from calibration  $\gamma$ -ray sources such as  ${}^{24}\text{Na}$ ,  ${}^{60}\text{Co}$ , and  ${}^{137}\text{Cs}$  acquired concurrently with the in-beam spectra were used to monitor the energy calibration of the spectra. The detector efficiencies and their small energy nonlinearities were calibrated using  ${}^{226}\text{Ra}$  and  ${}^{152}\text{Eu}$  radioactive sources.

The  $\gamma$ -ray excitation functions for  ${}^{106}\text{Pd}$  were measured at  $90^\circ$  with respect to the incident neutrons over a range of neutron energies from 2.0 to 3.8 MeV in 0.1 MeV increments. The  $\gamma$ -ray thresholds and shapes of the excitation functions were used to identify new levels and to place transitions in the level scheme supporting the coincidence analysis discussed below. The excitation function yields, corrected for  $\gamma$ -ray detection efficiency and multiple scattering, were compared to statistical model calculations using the code CINDY [13,14], which predicts the change in the cross sections as a function of bombarding energy and spin. Along with the angular-distribution data, the excitation functions also contribute to the determination of spins.

Angular distribution measurements were performed at incident neutron energies of 2.2, 2.7, and 3.5 MeV, where the detector was placed at angles between  $40^\circ$  and  $150^\circ$ . The variation of the yield of a particular  $\gamma$  ray as a function of the angle  $\theta$  was fit with a polynomial form related to the angle by the Legendre polynomial as

$$W(\theta) = A_0[1 + a_2 P_2(\cos \theta) + a_4 P_4(\cos \theta)], \quad (1)$$

where the angular distribution coefficients  $a_2$  and  $a_4$  depend on the level spins, multipolarities, and mixing ratios of transitions from the level;  $P_2(\cos \theta)$  and  $P_4(\cos \theta)$  are the Legendre polynomials. Level spins and multipole mixing ratios,  $\delta$ , were deduced by comparing the measured angular distributions with statistical model calculations. Branching ratios were also obtained from the angular distribution data. An example angular distribution and mixing ratio determination are shown in Fig. 1.

Level lifetimes were extracted from each of the three angular-distribution measurements using the Doppler-shift attenuation method (DSAM), as described in Refs. [15,16]. Examples of lifetimes determined in the present measurements are shown in Fig. 2. The spectral fitting was performed using the TV software package [17].

The spectra from the  $\gamma$ -ray angular distributions were also summed at each of the three incident neutron energies to improve the counting statistics. These high-statistics spectra were used to confirm the presence of low-intensity  $\gamma$  rays. An example spectrum to demonstrate the quality of the data is displayed in Fig. 3.

A  $\gamma$ - $\gamma$  coincidence measurement [18] was carried out at a neutron energy of 3.3 MeV with four HPGe detectors placed  $\approx 6$  cm from the center of the sample in a co-planar arrangement. Events were recorded when at least two detectors registered coincident events within a 100 ns time window. The data were sorted offline into  $4k \times 4k$  prompt and random-background matrices with 40 ns coincidence time gates. The random-background matrix was then subtracted from the prompt matrix, and the offline coincidence data analyses were performed using the RADWARE software package [19]. The  $\gamma$ - $\gamma$  coincidence data were used to build the level scheme of  ${}^{106}\text{Pd}$ , and also to determine the relative  $\gamma$ -ray intensities if

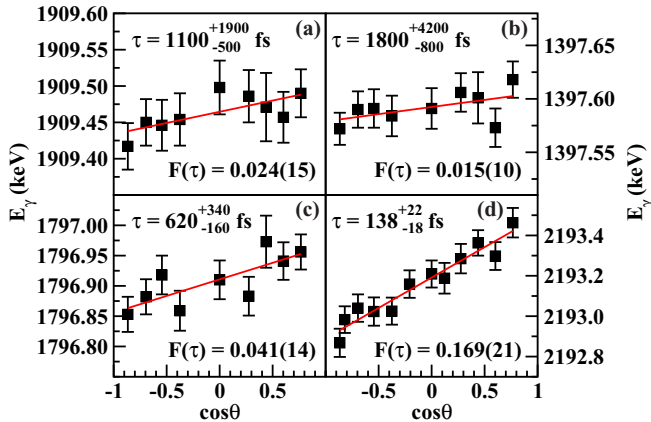


FIG. 2. Lifetimes from the Doppler-shift data for the (a) 1909.5 and (b) 1397.6 keV  $\gamma$  rays from the 1909.5 keV level, (c) the 1796.9 keV  $\gamma$  ray from the 2308.8 keV level, and (d) the 2193.3 keV  $\gamma$  ray from the 2705.2 keV level.

complex multiplets appeared in the singles spectra. Examples of gated  $\gamma$ - $\gamma$  coincidence spectra are shown in Fig. 4.

### III. RESULTS AND DISCUSSION

The results of the current work are presented in Tables I and II. Table I includes only information obtained in the current measurements. Table II includes some information from other sources, as documented in the table notes, when the values could not be obtained from our  $(n, n'\gamma)$  data. Low-lying states in  $^{106}\text{Pd}$ , arranged in a manner that permits assessment of its structure in terms of collective quadrupole excitations, are

shown in Fig. 5. The sources of the  $E2$  transition probabilities shown are documented in the notes of Table II.

#### A. Level discussions

There are three levels in the Nuclear Data Sheets (NDS) compilation [20] that should have been observed in our measurements but were not: the  $1904\ 2^-, 3^-$ ;  $2472\ 1^+, 2^+$ ; and  $2649\ 4^+$  levels. The  $\gamma$  rays from the 1904 keV state were reassigned to the 1910 keV level, based on energies and angular distributions. From the 2472 keV level, the 472, 766, and 1960 keV  $\gamma$  rays were not observed. Finally, the only branch from the 2649 keV level, the 1087 keV  $\gamma$  ray, was also not observed. We, therefore, refute the existence of these three levels.

A comment concerning the order of the  $4_3^+$  state and the  $6_1^+$  state is also warranted. In Table I, we show that the  $6_1^+$  state lies at 2076.8 keV and the  $4_3^+$  state at 2077.5 keV. Our reasoning for this assignment is primarily based on energies; the 949.5 and 1565.7 keV branches from the  $4_3^+$  level lead to a level energy of 2077.5 keV. The doublet around 848 keV yields  $\gamma$  rays at 847.4 and 848.3 keV. The latter is in agreement with the 2077.5 keV level energy, while the former represents the transition from the  $6_1^+$  level and accommodates a level at 2076.8 keV. This ordering of the two states is reversed, however, when compared with the most recent NDS compilation [20] but is in agreement with the previous version [24]. Moreover, these placements are also in agreement with the data from  $^{106m}\text{Ag}$  decay by Tivin *et al.* [25], who originally concluded the existence of the two levels. Few other measurements populate both the  $4_3^+$  and the  $6_1^+$  states, while quoting sufficiently small uncertainties on the energies to afford a comparison.

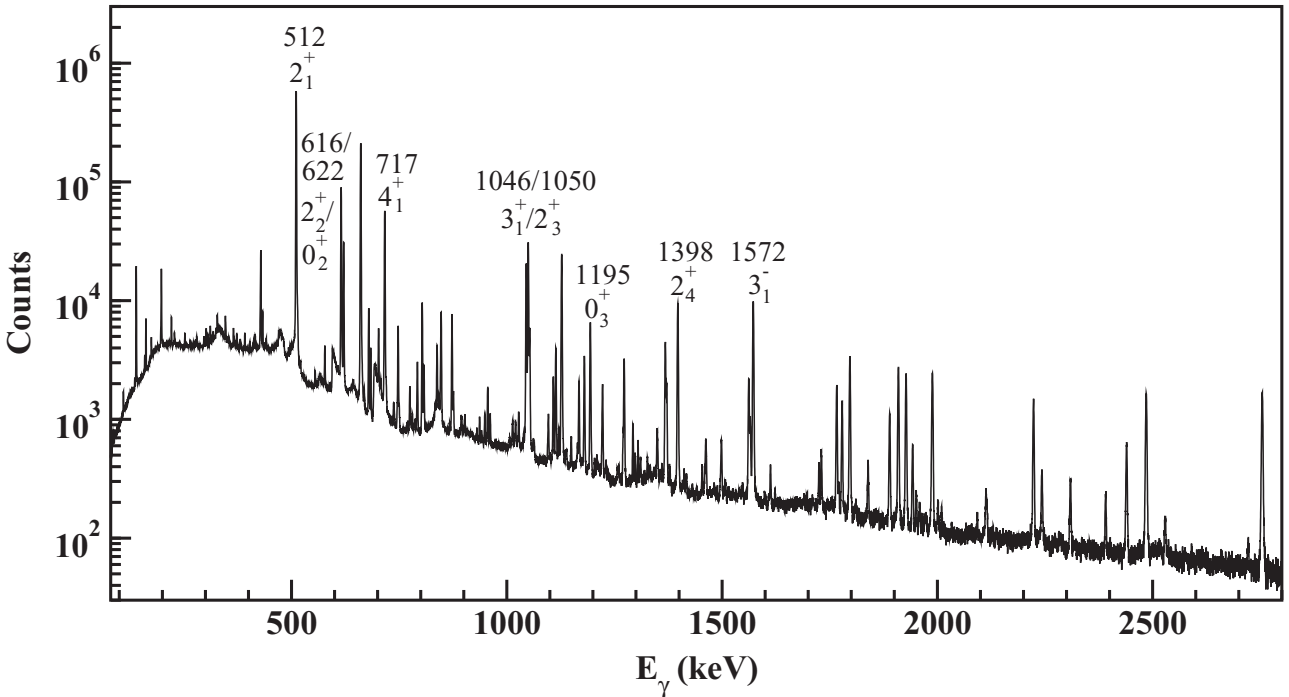


FIG. 3. Spectrum obtained by summing the  $\gamma$ -ray spectra for all angles for the  $E_n = 2.7$  MeV angular distribution. Some prominent peaks are labeled with the  $\gamma$ -ray energy, and level spin and parity.

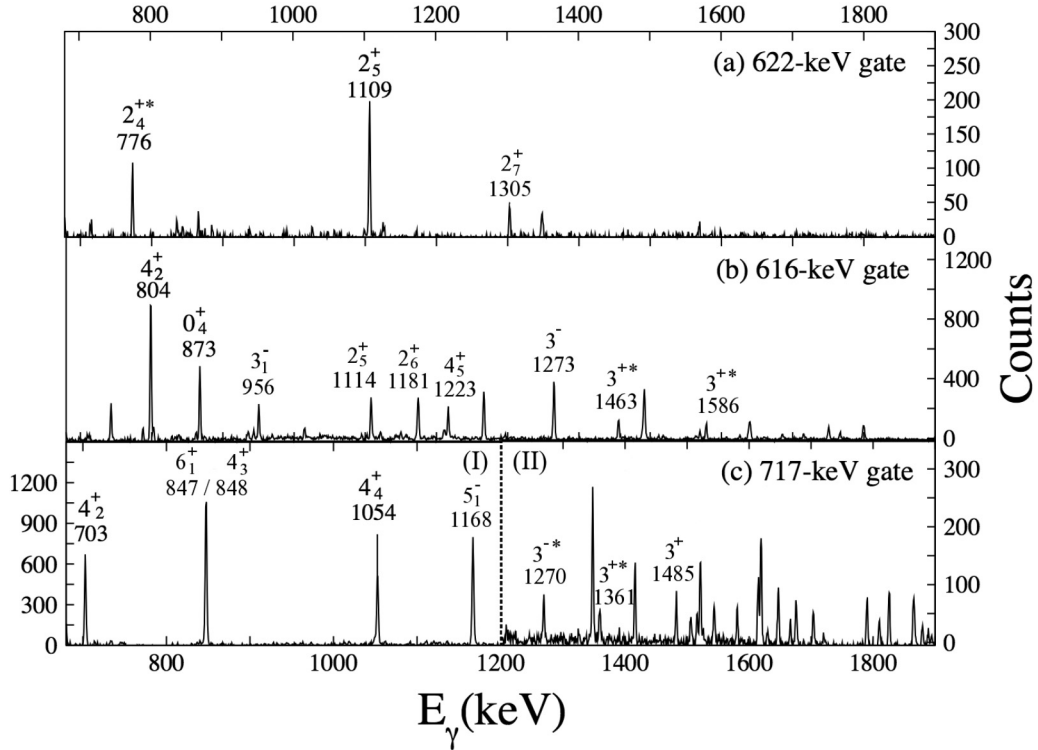


FIG. 4.  $\gamma$ - $\gamma$  coincidence spectra gated on the (a)  $0_2^+ \rightarrow 2_1^+$  622, (b)  $2_2^+ \rightarrow 2_1^+$  616, and (c)  $4_1^+ \rightarrow 2_1^+$  717 keV  $\gamma$  rays. The value of  $J_i^\pi$  is given above the labeled  $\gamma$ -ray energies only for the most intense  $\gamma$  rays with firm spin assignments. New  $\gamma$  rays from this work are marked with \*. The right-hand section of panel (c), (II), has an expanded  $y$  axis compared to the left-hand section, (I).

Four other levels are present in our level scheme as well as the current NDS compilation [20] for which we obtained contradictory information. First, for the 2500 keV level, the lifetime obtained from the 1988 keV  $\gamma$  ray is quite different than that obtained using the other branches. Yet, the coincidence data show a small peak at 1988 keV when gating on the 477 keV  $\gamma$  ray from the 2977 keV level. We, therefore, suggest that the 1988 keV  $\gamma$  ray is a doublet from two close-lying levels. Second, the spin of the 2579 keV level is given as ( $5^-$ ), but we find a branch to the first  $3^+$  state, negating this possible spin assignment as we do not expect to observe  $M2$  transitions in our measurements. Based on the angular distributions of the  $\gamma$  rays, we conclude that the spin is 4, but we cannot assign a parity. Third, the 2741 keV state was assigned [20] as  $J^\pi = 4^+$ , yet we observe the ground-state transition, limiting the spin and parity to  $1, 2^+$ . However, we do not observe the  $\gamma$  ray to the first excited state. Finally, the 3083 keV level is assigned a spin of 0, but we observed an anisotropic angular distribution for the 2572 keV  $\gamma$  ray as well as a new transition to the first  $3^+$  state and assign a spin of 3.

### B. Comparison of $B(E2)$ s with model predictions

The reduced transition probabilities obtained in the current work are presented in Table II. Svensson *et al.* [8,11] studied the low-spin structure of the heavy stable palladium isotopes by multistep Coulomb excitation, showing that vibrational degrees of freedom may be important for the description of the low-lying level structure of  $^{106}\text{Pd}$ . However, serious

discrepancies were found in the decay properties; most of the single-phonon transitions are smaller than predicted for a pure harmonic quadrupole vibrator. In many cases, the  $B(E2)$ s are too small by a factor of two or more. This discrepancy is notably true for the  $0_3^+ \rightarrow 2_2^+$  transition, which is weak and is inconsistent with a quadrupole vibrational picture. Thus, the primary focus of the present work is on the triplet of states with  $J^\pi(E_x \text{ in keV})$   $4_1^+(1229)$ ,  $2_2^+(1128)$ , and  $0_2^+(1134)$ , and the quintuplet of states with  $6_1^+(2077)$ ,  $4_2^+(1932)$ ,  $3_1^+(1558)$ ,  $2_3^+(1562)$ , and  $0_3^+(1706)$ .

The lack of  $E2$  strength is already evident for the purported two-phonon triplet. The  $B(E2)$  for each decay as predicted by the harmonic vibrator model should be 88 W.u., yet the experimentally determined values are considerably smaller. Two of the three  $B(E2)$ s are a factor of two smaller than the vibrational prediction. Effective field theory (EFT) calculations by Pérez and Papenbrock [26] also take into account possible anharmonicities and provide theoretical uncertainties for the labeled two-phonon decays in  $^{106}\text{Pd}$ . While their calculated  $B(E2)$  values agree with the experimental ones within error, the theoretical uncertainties are rather large, about 30%. Nonetheless, they suggest that  $^{106}\text{Pd}$  can be viewed as an anharmonic quadrupole vibrator at the two-phonon level.

Proceeding to the potential three-phonon states, the deficiency of  $E2$  strength is even more pronounced. If, however, it is assumed that the strength is fragmented over multiple states of the same spin and parity, it is useful to sum the  $E2$  strength into the candidate two-phonon states to evaluate this possibility. The summed  $E2$  strengths from all  $2^+$ ,  $3^+$ , and

TABLE I. Level and  $\gamma$ -ray energies, initial spins and parities, final spins and parities,  $\gamma$ -ray intensities, average experimental attenuation factors, level lifetimes, and multipolarity or  $E2/M1$  multipole mixing ratios,  $\delta$ , in  $^{106}\text{Pd}$  from the present inelastic neutron-scattering measurements only. When two  $\delta$  values with similar  $\chi^2$  values were deduced, the  $\delta$  with the lowest value of  $\chi^2$  is listed first. (The  $\gamma$ -ray and level energies for the  $2_1^+$  level, however, were taken from Ref. [20].) Levels and  $\gamma$  rays observed for the first time in this work are in **bold**. In cases where the  $\gamma$  ray was observed, but was contaminated by background or  $\gamma$  rays from other Pd isotopes and was weak in the coincidence spectra, the  $\gamma$ -ray energies are given without uncertainties and were calculated from level-energy differences and  $\gamma$ -ray intensities are given as upper limits or not at all.

$E_{\text{level}}$ (keV)	$E_\gamma$ (keV)	$J_i^\pi$	$J_f^\pi$	$I_\gamma$	$\bar{F}(\tau)$	$\tau$ (fs)	Multipolarity or $\delta$
511.850(23)	511.842(28)	$2_1^+$	$0_1^+$	100			$E2$
1128.103(16)	616.232(11)	$2_2^+$	$2_1^+$	100.0(30)	0.012(6)	$2300^{+2100}_{-800}$	$-8.7^{+17}_{-19}$
	1128.084(12)		$0_1^+$	54.6(16)			$E2$
1133.927(28)	622.038(11)	$0_2^+$	$2_1^+$	100			$E2$
1229.293(22)	717.410(11)	$4_1^+$	$2_1^+$	100	0.024(7)	$1140^{+440}_{-250}$	$E2$
1557.771(21)	328.479(25)	$3_1^+$	$4_1^+$	3.98(40)			
	429.661(13)		$2_2^+$	40.9(41)			$-8.8^{+9}_{-18}$
	1045.893(13)		$2_1^+$	100.0(30)			$-4.03^{+37}_{-45}$
1562.299(23)	333.00(13)	$2_3^+$	$4_1^+$	0.40(10)	0.020(7)	$1300^{+720}_{-350}$	$E2$
	428.339(22)		$0_2^+$	4.40(88)			$E2$
	434.196		$2_2^+$				
	1050.412(12)		$2_1^+$	100.0(30)			$+0.219^{+38}_{-44}$
	1562.295(25)		$0_1^+$	11.20(56)			$E2$
1706.424(30)	578.330(15)	$0_3^+$	$2_2^+$	16.70(84)	0.016(12)	$1600^{+5100}_{-700}$	$E2$
	1194.548(13)		$2_1^+$	100.0(30)			$E2$
1909.509(26)	<b>347.230(25)</b>	$2_4^+$	$2_3^+$	6.10(61)	0.017(8)	$1600^{+1500}_{-500}$	
	<b>351.81(13)</b>		$3_1^+$	0.93(28)			
	<b>680.201(16)</b>		$4_1^+$	7.50(38)			$E2$
	<b>775.576(22)</b>		$0_2^+$	5.50(28)			$E2$
	781.607(55)		$2_2^+$	1.50(15)			$+2.1^{+15}_{-8}$
	1397.642(18)		$2_1^+$	100.0(30)			$+0.253^{+55}_{-46}$
	1909.496(49)		$0_1^+$	46.4(23)			$+1.32^{+11}_{-15}$
1932.440(26)	374.669	$4_2^+$	$3_1^+$		0.017(12)	$1600^{+3500}_{-700}$	$E2$
	703.148(15)		$4_1^+$	39.0(20)			$-1.55^{+27}_{-66}$
	804.338(14)		$2_2^+$	100.0(30)			$E2$
2001.597(36)	873.494(15)	$0_4^+$	$2_2^+$	100		>1200	$E2$
2076.770(47)	847.434(20)	$6_1^+$	$4_1^+$	100			$E2$
2077.508(41)	848.252(23)	$4_3^+$	$4_1^+$	100(20)	0.095(84)	$270^{+2100}_{-140}$	$+0.20^{+14}_{-9}$
	949.507(90)		$2_2^+$	6.56(66)			$E2$
	1565.695(48)		$2_1^+$	25.6(51)			$E2$
2084.494(33)	522.195	$3_1^-$	$2_3^+$	<1.4	0.020(11)	$1400^{+1800}_{-500}$	$E1$
	956.388(26)		$2_2^+$	7.69(77)			$E1$
	1572.619(36)		$2_1^+$	100.0(30)			$E1$
2242.568(29)	680.269	$2_5^+$	$2_3^+$	98(15)	0.057(16)	$460^{+190a}_{-110}$	$-0.786^{+59}_{-68}$
	684.786(18)		$3_1^+$	48.4(24)			$+3.75^{+73}_{-67}$
	1108.632(24)		$0_2^+$	50.3(25)			$E2$
	1114.477(22)		$2_2^+$	100.0(30)			$+0.66^{+65}_{-33}$
	1730.707(50)		$2_1^+$	16.59(83)			$-0.03^{+12}_{-11}$
							$+2.5^{+11}_{-7}$

TABLE I. (*Continued.*)

$E_{\text{level}}$ (keV)	$E_{\gamma}$ (keV)	$J_i^{\pi}$	$J_f^{\pi}$	$I_{\gamma}$	$\bar{F}(\tau)$	$\tau$ (fs)	Multipolarity or $\delta$
	2242.746(94)		$0_1^+$	19.19(96)			$E2$
2278.212(98)	1766.362(40)	$0_5^+$	$2_1^+$	100			$E2$
2283.074(42)	<b>720.8(5)</b>	$4_4^+$	$2_3^+$	14.7(29)	0.022(15)	$1200^{+2600}_{-500}$	$E2$
	1053.776(21)		$4_1^+$	100.0(30)			$+0.170^{+54}_{-44}$
2306.181(31)	221.631(22)	$4_1^-$	$3_1^-$	32.0(64)			$E1$
	228.716(36)		$4_3^+$	13.4(27)			$E1$
	748.449(18)		$3_1^+$	100.0(30)			$E1$
2308.784(39)	<b>307.187</b>	$2_6^+$	$0_4^+$	<2	0.045(11)	$580^{+190}_{-120}$	$E2$
	<b>746.529(58)</b>		$2_3^+$	5.70(57)			$-0.15(26)$
	750.933(43)		$3_1^+$	5.20(52)			$-1.6^{+15}_{-20}$
	1180.691(23)		$2_2^+$	55.3(28)			$-0.4^{+3}_{-33}$
							$-0.22(4)$
	1796.926(41)		$2_1^+$	100.0(30)			$+5.1^{+12}_{-9}$
	2308.99(12)		$0_1^+$	11.3(11)			$+0.192^{+48}_{-50}$
2350.914(32)	418.27(20)	$4_5^+$	$4_2^+$	6.8(20)			$+1.48^{+14}_{-16}$
	793.133(21)		$3_1^+$	97.6(98)			$E2$
							$-8^{+3}_{-13}$
							$-0.085(90)$
	1121.416(49)		$4_1^+$	11.0(22)			$E2$
	1222.805(25)		$2_2^+$	100.0(30)			$E2$
	1839.146(62)		$2_1^+$	31.8(16)			$E2$
2366.107(41)	433.667	$5_1^+$	$4_2^+$	<3.7			$E2$
	808.341(21)		$3_1^+$	100.0(30)			$E2$
	1136.83(13)		$4_1^+$	5.7(11)			$E2$
2397.550(50)	<b>313.11(42)</b>	$5_1^-$	$3_1^-$	2.90(73)			$E2$
	1168.234(24)		$4_1^+$	100.0(30)			$E1$
2401.115(36)	<b>316.621(62)</b>	$2^-, 3^-$	$3_1^-$	6.3(13)			$E1$
	<b>838.817(22)</b>		$2_3^+$	90.7(45)			$E1$
	<b>843.344</b>		$3_1^+$	<12.9			$E1$
	1273.017(25)		$2_2^+$	100.0(30)			$E1$
	1889.231(55)		$2_1^+$	66.8(33)			$E1$
2439.111(44)	<b>876.766(29)</b>	$2_7^+$	$2_3^+$	15.3(15)	0.050(18)	$580^{+360}_{-170}$	$+0.01(16)$
							$+2.2^{+14}_{-1}$
	1209.770(91)		$4_1^+$	3.67(37)			$E2$
	1305.262(45)		$0_2^+$	7.57(76)			$E2$
	1927.271(58)		$2_1^+$	100.0(30)			$-0.055^{+39}_{-40}$
							$+2.74^{+34}_{-32}$
	2439.136(42)		$0_1^+$	30.8(15)			$E2$
2484.91(55)	2484.91(26)	$1^{(-)}$	$0_1^+$	100	0.185(18)	$120^{+16}_{-13}$	$(E1)$
2499.862(47)	<b>415.368</b>	$3^-$	$3_1^-$	<18	0.098(28)	$280^{+120}_{-70}$	
	<b>937.547(48)</b>		$2_3^+$	12.7(26)			$E1$
	942.18(10)		$3_1^+$	5.2(10)			$E1$
	<b>1270.460(64)</b>		$4_1^+$	17.9(36)			$E1$
	1371.751(29)		$2_2^+$	100(20)			$E1$

TABLE I. (*Continued.*)

$E_{\text{level}}$ (keV)	$E_{\gamma}$ (keV)	$J_i^{\pi}$	$J_f^{\pi}$	$I_{\gamma}$	$\bar{F}(\tau)$	$\tau$ (fs)	Multipolarity or $\delta$
	1988.012		$2_1^+$	<100			$E1$
<b>2500.126(54)</b>	<b>1988.256(11)</b>	2,3 $^+$	$2_1^+$	100	0.267(15)	$75_{-5}^{+6}$	
2578.689(40)	<b>181.068(42)</b>	4	$5_1^-$	27.9(56)			
	<b>272.504(59)</b>		$4_1^-$	19.1(19)			
	<b>494.082(38)</b>		$3_1^-$	47.7(48)			
	1020.900(35)		$3_1^+$	64.1(64)			
	1349.500(28)		$4_1^+$	100.0(30)			
2590.575(48)	<b>347.993(60)</b>	3 $^+$	$2_3^+$	19.0(19)			$-1.68(21)$
	658.1(1)		$4_2^+$	11.3(23)			$-0.342_{-54}^{+51}$
	<b>1028.201(33)</b>		$2_3^+$	100.0(30)			
	<b>1361.2(3)</b>		$4_1^+$	28.5(57)			
	<b>1462.557(32)</b>		$2_2^+$	57.0(57)			$+0.83_{-13}^{+20}$
	<b>2078.14(23)</b>		$2_1^+$	27.00(81)			
2624.424(79)	1062.197(49)	0 $_6^+$	$2_3^+$	81.2(81)			$E2$
	1496.232(74)		$2_2^+$	59.7(60)			$E2$
	2112.491(75)		$2_1^+$	100(10)			$E2$
2626.860(50)	1064.39(11)	(3) $^+$	$2_3^+$	7.9(16)	0.076(18)	$360_{-70}^{+120}$	$+0.05_{-15}^{+14}$
	1498.759(25)		$2_2^+$	100(20)			$+0.294_{-37}^{+31}$
	2115.050(58)		$2_1^+$	31.8(64)			$+0.394_{-86}^{+96}$
							$+5.7_{-20}^{+49}$
<b>2647.036(55)</b>	<b>737.5(2)</b>	(4) $^+$	$2_4^+$	6.7(20)	0.056(24)	$500_{-160}^{+410}$	$(E2)$
	<b>1089.350(78)</b>		$3_1^+$	24.0(24)			
	<b>1417.713(27)</b>		$4_1^+$	100.0(30)			
	<b>2135.365(78)</b>		$2_1^+$	11.3(23)			$(E2)$
2699.68(12)	302.130(49)	6 $_1^-$	$5_1^-$	100.0(50)			
	393.501		$4_1^-$	<42			
2705.211(97)	<b>998.87(15)</b>	1 $^+$	$0_3^+$	12.8(13)	0.171(18)	$145_{-17}^{+20}$	$M1$
	1571.3(2)		$0_2^+$	3.60(72)			$M1$
	1577.1(2)		$2_2^+$	28.3(57)			
	2193.340(48)		$2_1^+$	100.0(30)			
	2705.25(11)		$0_1^+$	52.1(52)			$M1$
2713.926(52)	1156.186(31)	3 $^+$	$3_1^+$	100.0(50)	0.069(27)	$400_{-120}^{+270}$	
	1484.6(2)		$4_1^+$	49.4(35)			
	<b>1585.786(36)</b>		$2_2^+$	71.0(71)			
	2202.026(11)		$2_1^+$	16.9(34)			
<b>2737.252(90)</b>	<b>659.7(2)</b>	(4) $^+$	$4_3^+$	100(20)			
	<b>1179.5(2)</b>		$3_1^+$	53(11)			
	<b>1507.959(41)</b>		$4_1^+$	43.0(43)			
2741.44(13)	2741.442(59)	1,2 $^+$	$0_1^+$	100			
2747.688(54)	<b>247.745(49)</b>	3	$3^-$	23.8(24)	0.058(46)	$500_{-200}^{+1800}$	
	<b>1518.473(39)</b>		$4_1^+$	23.1(23)			
	2235.808(33)		$2_1^+$	100.0(50)			
<b>2752.564(75)</b>	<b>668.1(2)</b>	(5)	$3_1^-$	6.6(20)			
	<b>674.917(90)</b>		$4_3^+$	6.4(19)			

TABLE I. (*Continued.*)

$E_{\text{level}}$ (keV)	$E_\gamma$ (keV)	$J_i^\pi$	$J_f^\pi$	$I_\gamma$	$\bar{F}(\tau)$	$\tau$ (fs)	Multipolarity or $\delta$
2757.08(11)	<b>1523.412(36)</b>		$4_1^+$	100(10)			
	406.177(86)		$4_5^+$	43.4(87)			
	450.889(63)		$4_1^-$	100(20)			
	824.637		$4_2^+$	<92			
2775.95(22)	1527.8(4)		$4_1^+$	30(15)			
	<b>1213.5(2)</b>	(3,4)	$2_3^+$	15.8(79)	0.092(47)	$290^{+330}_{-110}$	
	1217.9(3)		$3_1^+$	100.0(30)			
	1546.7(2)		$4_1^+$	33.6(67)			
	<b>1647.8(2)</b>		$2_2^+$	80(16)			
2783.88(11)	2264.101(98)		$2_1^+$	18.1(36)			
	2272.032(44)	2,3	$2_1^+$	100		$81^{+7}_{-6}$	
	<b>2812.270(68)</b>	(6 <sup>+</sup> )	$4_3^+$	26.8(80)			(E2)
2820.49(10)	<b>734.804(84)</b>		$4_2^+$	39.4(79)			(E2)
	<b>879.830(55)</b>		$4_1^+$	100(10)			(E2)
	<b>1582.968(40)</b>		$2_3^+$	11.4(34)	0.091(25)	$290^{+120}_{-70}$	+1.4 <sup>+64</sup> -58
2828.393(89)	1258.2(3)	2 <sup>+</sup>	$2_1^+$	17.2(52)			+0.22 <sup>+31</sup> -17
	1692.4(2)		$2_2^+$	100.0(50)			-0.18(10)
	2308.6(2)		$2_1^+$				+4 <sup>+12</sup> -2
	2820.494(47)		$0_1^+$	53.1(53)			+2.36 <sup>+42</sup> -40
2846.168(92)	1266.053(80)	(0 <sup>+</sup> )	$2_3^+$	18.1(36)	0.089(32)	$300^{+180}_{-90}$	(E2)
	2316.558(43)		$2_1^+$	100.0(30)			(E2)
	<b>1283.91(10)</b>		$2_3^+$	8.3(17)	0.088(27)	$300^{+150}_{-80}$	
2850.766(52)	<b>1616.867(46)</b>		$4_1^+$	100.0(70)			
	<b>918.412(75)</b>	3	$4_3^+$	12.2(24)	0.147(23)	$170^{+37}_{-27}$	
	<b>941.3(2)</b>		$2_4^+$	18.9(28)			
	1621.468(26)		$4_1^+$	100.0(30)			
2860.30(20)	<b>1722.631(60)</b>		$2_2^+$	19.9(40)			
	<b>775.80(20)</b>		$3_1^-$	100			
	1302.932(35)	(5 <sup>+</sup> )	$3_1^+$	100(15)			(E2)
2875.728(88)	1632.281(63)		$4_1^+$	54(11)			
	<b>1646.435(40)</b>		$4_1^+$	100			
	1315.757(98)		$2_3^+$	12.0(24)	0.034(30)	$800^{+6400}_{-400}$	
2878.377(78)	2366.137(42)		$2_1^+$	100.0(70)			
	<b>1320.63(11)</b>		$3_1^+$	10.3(10)	0.071(34)	$380^{+370}_{-130}$	
	<b>1649.082(37)</b>		$4_1^+$	100(10)			
2886.239(56)	<b>1758.115(32)</b>	(3)	$2_2^+$	100.0(70)	0.083(18)	$323^{+99}_{-63}$	
	2374.429(37)		$2_1^+$	61.2(43)			
2897.454(70)	<b>591.3(2)</b>	4,5 <sup>-</sup>	$4_1^-$	43(11)	0.074(34)	$360^{+330}_{-120}$	
	<b>813.74(10)</b>		$3_1^-$	26.5(40)			
	1668.082(33)		$4_1^+$	100.0(30)			
2902.476(75)	1774.299(57)	1,2 <sup>+</sup>	$2_2^+$	$\leq 16$	0.254(16)	$87^{+8}_{-7}$	
	2390.626		$2_1^+$	$\leq 100$			
	2902.476		$0_1^+$	$\leq 3$			

TABLE I. (*Continued.*)

$E_{\text{level}}$ (keV)	$E_{\gamma}$ (keV)	$J_i^{\pi}$	$J_f^{\pi}$	$I_{\gamma}$	$\bar{F}(\tau)$	$\tau$ (fs)	Multipolarity or $\delta$
<b>2907.516(88)</b>	<b>1678.223(40)</b>		$4_1^+$	100	0.050(48)	>270	
2908.651(64)	<b>824.329(48)</b>		$3_1^-$	16.7(33)	0.069(20)	$390^{+180}_{-90}$	
	<b>1346.080(83)</b>		$3_1^+$	9.3(28)			
	2396.742(34)		$2_1^+$	100.0(50)			
2917.997(89)	1355.7(2)	$2^+$	$2_3^+$	4.4(13)	0.213(18)	$109^{+12}_{-11}$	
	1360.2(2)		$3_1^+$	18.7(28)			
	2406.134(37)		$2_1^+$	100.0(70)			$-0.047^{+31}_{-63}$ $+2.66^{+59}_{-44}$
	2918.16(16)		$0_1^+$	7.3(11)			<i>E2</i>
2935.518(48)	<b>1706.010(43)</b>	(3)	$4_1^+$	20.5(31)	0.230(15)	$99^{+9}_{-8}$	
	<b>1807.251(33)</b>		$2_2^+$	37.4(56)			
	2424.101(33)		$2_1^+$	100.0(50)			
2968.52(13)	2456.670(56)		$2_1^+$	100			
<b>2970.73(13)</b>	<b>2458.875(54)</b>		$2_1^+$	100			
<b>2976.699(80)</b>	<b>476.9(2)</b>		$3^-$	36(11)	0.187(48)	$127^{+54}_{-31}$	
	<b>892.205(34)</b>		$3_1^-$	100			
<b>3022.042(72)</b>	<b>1792.749(32)</b>		$4_1^+$	100	0.236(28)	$95^{+16}_{-13}$	
3037.27(19)	1909.165	1	$2_2^+$	24(12)	0.459(25)	$35^{+4}_{-3}$	
	3037.268(90)		$0_1^+$	100.0(50)			<i>M1 or E1</i>
<b>3041.60(19)</b>	<b>758.42(10)</b>	(6 $^+$ )	$4_4^+$	20.6(41)			<i>(E2)</i>
	<b>1812.61(18)</b>		$4_1^+$	100.0(50)			<i>(E2)</i>
3054.43(33)	<b>1920.5(2)</b>	(1)	$0_2^+$	13.2(33)	0.242(42)	$92^{+25}_{-18}$	
	<b>1926.3(2)</b>		$2_2^+$	12.0(60)			
	2542.6(2)		$2_1^+$	100.0(70)			
	3054.43(16)		$0_1^+$	11.0(11)			
<b>3057.688(72)</b>	<b>1828.395(32)</b>	(3)	$4_1^+$	100.0(50)	0.132(32)	$190^{+69}_{-42}$	
	<b>1929.6(2)</b>		$2_2^+$	33(10)			
	<b>2545.8(2)</b>		$2_1^+$	35(10)			
<b>3067.364(78)</b>	<b>1939.262(48)</b>		$2_2^+$	66(10)	0.123(55)	$210^{+190}_{-70}$	
	<b>2555.512(50)</b>		$2_1^+$	100(15)			
3071.057(97)	2559.207(39)		$2_1^+$	100			
3083.343(95)	<b>1525.6(2)</b>	(3)	$3_1^+$	74(19)	0.108(34)	$240^{+120}_{-60}$	
	1955.2(2)		$2_2^+$	11.9(24)			
	2571.492(38)		$2_1^+$	100.0(50)			
3097.485(70)	<b>1868.192(31)</b>		$4_1^+$	100			
<b>3110.83(16)</b>	<b>2598.974(75)</b>	1,2 $^+$	$2_1^+$	100(15)			
	<b>3110.88(21)</b>		$0_1^+$	38.3(57)			
3121.27(15)	2609.416(65)		$2_1^+$	100	0.138(52)	$180^{+130}_{-60}$	
3161.11(14)	<b>1076.5(3)</b>	(2,3)	$3_1^-$	28.9(29)	0.283(85)	$74^{+43}_{-23}$	
	2649.260(59)		$2_1^+$	100(10)			
3166.28(13)	<b>2032.4(2)</b>	1	$0_2^+$	79(12)	0.176(53)	$135^{+70}_{-38}$	<i>M1 or E1</i>
	2654.4(2)		$2_1^+$	86(26)			
	3166.281(61)		$0_1^+$	100.0(70)			<i>M1 or E1</i>
3173.723(73)	2045.408(42)		$2_2^+$	100(25)	0.082(33)	$320^{+240}_{-100}$	
	<b>2662.261(52)</b>		$2_1^+$	86.9(87)			

TABLE I. (*Continued.*)

$E_{\text{level}}$ (keV)	$E_{\gamma}$ (keV)	$J_i^{\pi}$	$J_f^{\pi}$	$I_{\gamma}$	$\bar{F}(\tau)$	$\tau$ (fs)	Multipolarity or $\delta$
<b>3215.041(92)</b>	<b>1652.742(42)</b>		$2_3^+$	100	0.089(47)	$290^{+350}_{-110}$	
3221.50(10)	2093.397		$2_2^+$	<100	0.148(70)	$160^{+170}_{-60}$	
	2709.624(78)		$2_1^+$	100(3)			
3249.56(14)	3249.556(65)	1,2 <sup>+</sup>	$0_1^+$	100	0.514(34)	28(4)	
3250.47(20)	2738.618(90)		$2_1^+$	100	0.41(10)	$43^{+21}_{-13}$	
3272.91(18)	3272.914(84)	1,2 <sup>+</sup>	$0_1^+$	100	0.725(53)	12(3)	
<b>3274.35(19)</b>	<b>2762.495(84)</b>		$2_1^+$	100			
3300.222(97)	<b>1737.906(61)</b>	1,2 <sup>+</sup>	$2_3^+$	27.0(40)	0.217(47)	$103^{+36}_{-23}$	
	<b>2172.09(25)</b>		$2_2^+$	100(15)			
	2788.357(71)		$2_1^+$	34(10)			
	<b>3300.45(18)</b>		$0_1^+$	52.9(79)			
3321.38(25)	2809.53(11)		$2_1^+$	100			

<sup>a</sup>This lifetime differs from the value published in Ref. [10]. We chose to apply a more stringent set of conditions for accepting the  $F(\tau)$  values extracted from each  $\gamma$  ray, which excluded all branches except the 1114.5 keV  $\gamma$  ray. The resulting lifetime has smaller uncertainties, but the error bars do overlap with the previously published value.

$4^+$  states above the candidate two-phonon  $0^+$ ,  $2^+$ , and  $4^+$  states, up to an excitation energy of 2.4 MeV, are presented in Table III. Figures 4(a)–4(c) show coincidence spectra, taken at a neutron bombarding energy of 3.3 MeV, from which one can assess feeding intensities to the triplet of states,  $0^+(1134)$ ,  $2^+(1128)$ , and  $4^+(1229)$  gated by their decays to the  $2^+(512)$  state via  $\gamma$  rays of 622, 616, and 717 keV, respectively. Table III shows the summing of  $B(E2; 2_i^+ \rightarrow 0_2^+)$ ,  $B(E2; 2_i^+ \rightarrow 2_2^+)$ ,  $B(E2; 4_i^+ \rightarrow 2_2^+)$ ,  $B(E2; 3_i^+ \rightarrow 2_2^+)$ ,  $B(E2; 2_i^+ \rightarrow 4_1^+)$ ,  $B(E2; 4_i^+ \rightarrow 4_1^+)$ , and  $B(E2; 3_i^+ \rightarrow 4_1^+)$  values (in W.u.) compared with the harmonic quadrupole vibrator for a three-phonon triplet. It is evident, by summing  $B(E2)$  values for the transitions feeding the candidate two-phonon triplet of states, that  $^{106}\text{Pd}$  is not a good case for a quadrupole vibrational nucleus. While a quintuplet of levels with appropriate spins is present and the decay patterns qualitatively reflect those of a three-phonon quintuplet, their decay strengths are inadequate for this to be a credible interpretation. Clearly, a deficit in  $E2$  strength exists in all cases, except possibly for the  $2_i^+ \rightarrow 0_2^+$  and  $2_i^+ \rightarrow 2_2^+$  summed transitions, and we must conclude that even fragmentation into high-lying states cannot account for the observed deficiency. The EFT calculations by Pérez and Papenbrock [26] also provided a “break down point” for the three-phonon states. The results presented here raise the question “What is the nature of collective quadrupole behavior in  $^{106}\text{Pd}$  and, more generally, how can we describe the nuclear structure in this mass region?”

To further explore the possible collective structure of  $^{106}\text{Pd}$ , we considered the other limiting cases of the Bohr model in addition to the harmonic quadrupole vibrator. The summed  $E2$  strength patterns compared to the (Wilets–Jean) gamma-soft rotor and rigid axially asymmetric rotor limits of the Bohr model are shown in Table III, respectively. We also show the summed  $E2$  strength compared to a proton-neutron interacting

boson model (IBM2) calculation. The IBM2 calculations were carried out with parameters very close to those used by Kim *et al.* [27].

Other IBM calculations are available, but contribute less data for a detailed comparison. For example, calculations by Böyükata *et al.* [28] provide potential-energy surfaces indicating that the structure of  $^{106}\text{Pd}$  may be more spherical in nature, but offer few  $B(E2)$  values for  $^{106}\text{Pd}$  specifically; no discussion of the nature of this individual nucleus is given. Prior calculations by Van Isacker *et al.* [29], however, provide additional  $B(E2)$  values on which the authors base the conclusion that the  $0_2^+$  state is not a member of an intruder band. Our interpretation of this state in particular is discussed in Sec. III C.

The comparisons of the experimental summed  $B(E2)$  values with the various models shown in Table III suggest that the collective character lies closest to an axially asymmetric rotor, with possibly some gamma softness. This conclusion is implicit in the IBM2 calculations as revealed in the closeness of the IBM2 calculated  $B(E2)$  values to the Wilets–Jean values. It is well known that, for large boson numbers, the IBM SO(6) limiting case can closely resemble the Wilets–Jean limit of the Bohr model.

In addition to the  $B(E2)$  values discussed above,  $B(M1)$  values in  $^{106}\text{Pd}$  have been discussed using IBM2 calculations by Kim *et al.* [27] and by Giannatiempo *et al.* [30]. Indeed, the issue of  $M1$  strengths was a major component of the paper by Kim *et al.*, and it was the focus of the paper by Giannatiempo *et al.*. We note that the two sets of calculations used very different parameter sets but obtained very similar results for the strongest  $M1$  (as well as  $E2$ ) transitions. We are unable to offer an explanation for this result beyond the observation that both sets of calculations involve a large number of parameters and there are probably multiple local fitting minima in this parameter space. However, we are able to deduce  $B(M1)$  values that critically impact these two sets of calculations.

TABLE II. Levels,  $\gamma$  rays, initial spins and parities, final spins and parities,  $\gamma$ -ray branching ratios, level lifetimes, and multipolarities or  $E2/M1$  multipole mixing ratios used to calculate transition probabilities in  $^{106}\text{Pd}$ . Values not obtained from the present measurements are labeled with superscripts and described in the footnotes.

$E_{\text{level}}$ (keV)	$E_{\gamma}$ (keV)	$J_i^{\pi}$	$J_f^{\pi}$	B. R.	$\tau$ (fs)	Multipolarity or $\delta$	$B(E2)$ (W.u.)	$B(E1)/B(M1)$ (W.u.)/( $\mu_N^2$ )
511.8	511.8	$2_1^+$	$0_1^+$	1.000	17600(900) <sup>a</sup>	$E2$	44.3(15) <sup>a</sup>	
1128.1	616.2	$2_2^+$	$2_1^+$	0.647(24)	4500(360) <sup>a</sup>	$-8.7_{-19}^{+17}$	$43.7_{-50}^{+58}$	$(4.6_{-18}^{+33}) \times 10^{-4}$
	1128.1		$0_1^+$	0.353(13)		$E2$	$1.18_{-13}^{+15}$	
1133.9	622.0	$0_2^+$	$2_1^+$	1.000	8400(1900) <sup>a</sup>	$E2$	35(8) <sup>a</sup>	
1229.3	717.4	$4_1^+$	$2_1^+$	1.000	1890(260) <sup>a</sup>	$E2$	76(11) <sup>a</sup>	
1557.8	328.5	$3_1^+$	$4_1^+$	0.027(3)	32000(2000) <sup>b</sup>		$6.0_{-60}^{+11}\text{c}$	
	429.7		$2_2^+$	0.282(30)		$-7.9(8)\text{a}$	$16.2_{-26}^{+30}$	$(10.0_{-30}^{+45}) \times 10^{-5}$
	1045.9		$2_1^+$	0.690(32)		$-4.03_{-45}^{+37}$	$0.444_{-50}^{+57}$	$(6.2_{-17}^{+21}) \times 10^{-5}$
1562.3	333.0	$2_3^+$	$4_1^+$	0.003(1)	1900(190) <sup>d</sup>	$E2$	$10.6_{-42}^{+51}$	
	428.3		$0_2^+$	0.038(8)		$E2$	$38_{-11}^{+13}$	
	434.2		$2_2^+$	0.011(1) <sup>a</sup>			$10_{-10}^{+2}\text{c}$	
	1050.4		$2_1^+$	0.853(34)		$+0.24(1)\text{a}$	$0.52_{-10}^{+13}$	$(2.08_{-27}^{+33}) \times 10^{-2}$
	1562.3		$0_1^+$	0.095(5)		$E2$	$0.147_{-20}^{+25}$	
1706.4	578.3	$0_3^+$	$2_2^+$	0.143(8)	4000(700) <sup>a</sup>	$E2$	$15.1_{-30}^{+42}$	
	1194.5		$2_1^+$	0.857(34)		$E2$	$2.41_{-44}^{+63}$	
1909.5	347.2	$2_4^+$	$2_3^+$	0.036(4)	$1600_{-500}^{+1500}$		$120_{-120}^{+80}\text{c}$	
	351.8		$3_1^+$	0.006(2)			$16_{-16}^{+18}\text{c}$	
	680.2		$4_1^+$	0.045(2)		$E2$	$5.2_{-27}^{+29}$	
	775.6		$0_2^+$	0.033(2)		$E2$	$2.0_{-10}^{+12}$	
	781.6		$2_2^+$	0.009(1)		$+2.1_{-8}^{+15}$	$0.44_{-28}^{+39}$	$(1.3_{-10}^{+29}) \times 10^{-4}$
	1397.6		$2_1^+$	0.595(23)		$+0.253_{-46}^{+55}$	$0.12_{-8}^{+14}$	$(7.3_{-38}^{+42}) \times 10^{-3}$
						$+1.32_{-15}^{+11}$	$1.21_{-66}^{+77}$	$(2.8_{-16}^{+22}) \times 10^{-3}$
	1909.5		$0_1^+$	0.276(15)		$E2$	$0.19_{-10}^{+11}$	
1932.4	374.7	$4_2^+$	$3_1^+$	0.015(2) <sup>a</sup>	1670(230) <sup>a</sup>		$33_{-33}^{+11}\text{c}$	
	703.1		$4_1^+$	0.276(16)		$-2.30(2)\text{a}$	$22.1_{-39}^{+51}$	$(4.3_{-8}^{+11}) \times 10^{-3}$
	804.3		$2_2^+$	0.709(28)		$E2$	$34.5_{-54}^{+71}$	
2001.6	873.5	$0_4^+$	$2_2^+$	1.000	>1200	$E2$	<45	
2076.8	847.4 <sup>e</sup>	$6_1^+$	$4_1^+$	1.000	710(70) <sup>a</sup>	$E2$	$88.3_{-79}^{+97}$	
2077.5	848.3	$4_3^+$	$4_1^+$	0.76(19)	$270_{-140}^{+2100}$	$+0.20_{-9}^{+14}$	$7_{-6}^{+41}$	$0.25_{-23}^{+42}$
	949.5		$2_2^+$	0.050(9)		$E2$	$7_{-6}^{+10}$	
	1565.7		$2_1^+$	0.194(49)		$E2$	$2.1_{-19}^{+34}$	
2084.5	522.2	$3_1^-$	$2_3^+$	0.013(3) <sup>a</sup>	$1400_{-500}^{+1800}$	$E1$		$(2.8_{-19}^{+27}) \times 10^{-5}$
	956.4		$2_2^+$	0.070(7)		$E1$		$(2.5_{-15}^{+18}) \times 10^{-5}$
	1572.6		$2_1^+$	0.916(38)		$E1$		$(7.3_{-43}^{+47}) \times 10^{-5}$
2242.6	680.3	$2_5^+$	$2_3^+$	0.294(46)	$460_{-110}^{+190}$	$-0.786_{-68}^{+59}$	$46_{-22}^{+31}$	$(4.2_{-32}^{+43}) \times 10^{-2}$
	684.8		$3_1^+$	0.146(10)		$+3.75_{-67}^{+73}$	$54_{-20}^{+23}$	$(3.8_{-20}^{+38}) \times 10^{-3}$
	1108.6		$0_2^+$	0.151(10)		$E2$	$5.4_{-19}^{+21}$	
	1114.5		$2_2^+$	0.301(17)		$+0.66_{-33}^{+65}$	$3.2_{-25}^{+50}$	$(1.9_{-11}^{+15}) \times 10^{-2}$
	1730.7		$2_1^+$	0.050(3)		$-0.03_{-11}^{+12}$	$0.0002_{-2}^{+52}$	$(1.20_{-42}^{+47}) \times 10^{-3}$
						$+2.5_{-7}^{+11}$	$0.167_{-69}^{+83}$	$(1.7_{-11}^{+22}) \times 10^{-4}$
	2242.7		$0_1^+$	0.058(4)		$E2$	$0.062_{-21}^{+25}$	
2278.2	715.9 <sup>a</sup>	$0_5^+$	$2_3^+$	0.226(11) <sup>a</sup>		$E2$		
	1766.4		$2_1^+$	0.774(30) <sup>a</sup>		$E2$		

TABLE II. (*Continued.*)

<i>E</i> <sub>level</sub> (keV)	<i>E</i> <sub><math>\gamma</math></sub> (keV)	<i>J</i> <sub><math>i</math></sub> <sup><math>\pi</math></sup>	<i>J</i> <sub><math>f</math></sub> <sup><math>\pi</math></sup>	B. R.	$\tau$ (fs)	Multipolarity or $\delta$	<i>B</i> ( <i>E</i> 2) (W.u.)	<i>B</i> ( <i>E</i> 1)/ <i>B</i> ( <i>M</i> 1) (W.u.)/( $\mu_N^2$ )
2283.1	720.8	4 <sub>4</sub> <sup>+</sup>	2 <sub>3</sub> <sup>+</sup>	0.128(26)	1200 <sub>-500</sub> <sup>+2600</sup>	<i>E</i> 2	15 <sub>-11</sub> <sup>+16</sup>	$(3.5_{-24}^{+28}) \times 10^{-2}$
	1053.8		4 <sub>1</sub> <sup>+</sup>	0.872(41)		+0.170 <sub>-44</sub> <sup>+54</sup>		
2306.2	221.6	4 <sub>1</sub> <sup>-</sup>	3 <sub>1</sub> <sup>-</sup>	0.220(45)				
	228.7		4 <sub>3</sub> <sup>+</sup>	0.092(19)		<i>E</i> 1		
	748.4		3 <sub>1</sub> <sup>+</sup>	0.688(41)		<i>E</i> 1		
2308.8	307.2	2 <sub>6</sub> <sup>+</sup>	0 <sub>4</sub> <sup>+</sup>	<0.011	580 <sub>-120</sub> <sup>+190</sup>	<i>E</i> 2	<191	$[7.4(30)] \times 10^{-3}$
	746.5		2 <sub>3</sub> <sup>+</sup>	0.032(3)		-0.15(26)		
	750.9		3 <sub>1</sub> <sup>+</sup>	0.029(3)		-1.6 <sub>-20</sub> <sup>+15</sup>		
	1180.7		2 <sub>2</sub> <sup>+</sup>	0.308(17)		-0.4 <sub>-33</sub> <sup>+3</sup>		
	1796.9		2 <sub>1</sub> <sup>+</sup>	0.557(21)		-0.22(4)	0.29 <sub>-15</sub> <sup>+24</sup>	$(1.76_{-53}^{+61}) \times 10^{-2}$
						+5.1 <sub>-9</sub> <sup>+12</sup>	6.1 <sub>-19</sub> <sup>+21</sup>	$(6.8_{-36}^{+65}) \times 10^{-4}$
						+0.192 <sub>-50</sub> <sup>+48</sup>	0.050 <sub>-30</sub> <sup>+50</sup>	$(9.1_{-27}^{+30}) \times 10^{-3}$
						+1.48 <sub>-16</sub> <sup>+14</sup>	0.97 <sub>-32</sub> <sup>+37</sup>	$(3.0_{-11}^{+15}) \times 10^{-3}$
	2309.0		0 <sub>1</sub> <sup>+</sup>	0.063(6)		<i>E</i> 2	0.046 <sub>-15</sub> <sup>+17</sup>	
2350.9	418.3	4 <sub>5</sub> <sup>+</sup>	4 <sub>2</sub> <sup>+</sup>	0.028(8)				
	793.1		3 <sub>1</sub> <sup>+</sup>	0.395(43)		-8 <sub>-13</sub> <sup>+3</sup>		
						-0.085(90)		
	1121.4		4 <sub>1</sub> <sup>+</sup>	0.044(9)				
	1222.8		2 <sub>2</sub> <sup>+</sup>	0.405(21)		<i>E</i> 2		
	1839.1		2 <sub>1</sub> <sup>+</sup>	0.129(9)		<i>E</i> 2		
2366.1	433.7	5 <sub>1</sub> <sup>+</sup>	4 <sub>2</sub> <sup>+</sup>	<0.034				
	808.3		3 <sub>1</sub> <sup>+</sup>	0.914(38)		<i>E</i> 2		
	1136.8		4 <sub>1</sub> <sup>+</sup>	0.052(11)				
2397.6	313.1	5 <sub>1</sub> <sup>-</sup>	3 <sub>1</sub> <sup>-</sup>	0.028(7)		<i>E</i> 2		
	1168.2		4 <sub>1</sub> <sup>+</sup>	0.972(41)		<i>E</i> 1		
2401.1	316.6	2 <sup>-</sup> , 3 <sup>-</sup>	3 <sub>1</sub> <sup>-</sup>	0.023(5)				
	838.8		2 <sub>3</sub> <sup>+</sup>	0.328(18)		<i>E</i> 1		
	843.3		3 <sub>1</sub> <sup>+</sup>	<0.047		<i>E</i> 1		
	1273.0		2 <sub>2</sub> <sup>+</sup>	0.361(14)		<i>E</i> 1		
	1889.2		2 <sub>1</sub> <sup>+</sup>	0.241(13)		<i>E</i> 1		
2439.1	876.8	2 <sub>7</sub> <sup>+</sup>	2 <sub>3</sub> <sup>+</sup>	0.097(10)	580 <sub>-170</sub> <sup>+360</sup>	+0.01(16)	0.001 <sub>-1</sub> <sup>+390</sup>	$(1.42_{-66}^{+78}) \times 10^{-2}$
						+2.2 <sub>-1</sub> <sup>+14</sup>	7.4 <sub>-34</sub> <sup>+54</sup>	$(2.4_{-19}^{+16}) \times 10^{-3}$
	1209.8		4 <sub>1</sub> <sup>+</sup>	0.023(2)		<i>E</i> 2	0.42 <sub>-18</sub> <sup>+22</sup>	
	1305.3		0 <sub>2</sub> <sup>+</sup>	0.048(5)		<i>E</i> 2	0.60 <sub>-27</sub> <sup>+33</sup>	
	1927.3		2 <sub>1</sub> <sup>+</sup>	0.635(24)		-0.055 <sub>-40</sub> <sup>+39</sup>	0.003 <sub>-3</sub> <sup>+11</sup>	$(8.7_{-36}^{+40}) \times 10^{-3}$
						+2.74 <sub>-32</sub> <sup>+34</sup>	1.00 <sub>-43</sub> <sup>+49</sup>	$(1.03_{-53}^{+83}) \times 10^{-3}$
	2439.1		0 <sub>1</sub> <sup>+</sup>	0.196(11)		<i>E</i> 2	0.108 <sub>-45</sub> <sup>+52</sup>	
2484.9	2484.9	1 <sup>(-)</sup>	0 <sub>1</sub> <sup>+</sup>	1.000	120 <sub>-13</sub> <sup>+16</sup>		(E1)	
	2499.9	415.4	3 <sup>-</sup>	<0.071		280 <sub>-70</sub> <sup>+120</sup>		
	937.5		2 <sub>3</sub> <sup>+</sup>	$\geq 0.050(11)$		<i>E</i> 1		$>(9.6_{-43}^{+59}) \times 10^{-5}$
	942.2		3 <sub>1</sub> <sup>+</sup>	$\geq 0.020(4)$		<i>E</i> 1		$>(3.8_{-17}^{+22}) \times 10^{-5}$
	1270.5		4 <sub>1</sub> <sup>+</sup>	$\geq 0.071(15)$		<i>E</i> 1		$>(5.5_{-24}^{+33}) \times 10^{-5}$
	1371.8		2 <sub>2</sub> <sup>+</sup>	$\geq 0.394(85)$		<i>E</i> 1		$>(2.4_{-11}^{+15}) \times 10^{-4}$
	1988.0 <sup>f</sup>		2 <sub>1</sub> <sup>+</sup>	<0.394		<i>E</i> 1		$<7.9 \times 10^{-5}$

TABLE II. (*Continued.*)

$E_{\text{level}}$ (keV)	$E_{\gamma}$ (keV)	$J_i^{\pi}$	$J_f^{\pi}$	B. R.	$\tau$ (fs)	Multipolarity or $\delta$	$B(E2)$ (W.u.)	$B(E1)/B(M1)$ (W.u.)/( $\mu_N^2$ )
2500.1	1988.3 <sup>f</sup>		$2_1^+$	1.000	$75_{-5}^{+6}$			
2578.7	181.1	4	$5_1^-$	0.108(22)				
	272.5		$4_1^-$	0.074(8)				
	494.1		$3_1^-$	0.184(20)				
	1020.9		$3_1^+$	0.248(27)				
	1349.5		$4_1^+$	0.386(19)				
2590.6	348.0	3 <sup>+</sup>	$2_5^+$	0.078(8)				
	658.1		$4_2^+$	0.047(9)				
	1028.2		$2_3^+$	0.412(20)		$-1.68(21)$		
	1361.2		$4_1^+$	0.117(24)		$-0.342_{-54}^{+51}$		
	1462.6		$2_2^+$	0.235(25)		$+0.83_{-13}^{+20}$		
	2078.1		$2_1^+$	0.111(5)				
2624.4	1062.2	0 <sub>6</sub> <sup>+</sup>	$2_3^+$	0.337(39)		$E2$		
	1496.2		$2_2^+$	0.248(29)		$E2$		
	2112.5		$2_1^+$	0.415(48)		$E2$		
2626.9	1064.4	(3) <sup>+</sup>	$2_3^+$	0.057(14)	$360_{-70}^{+120}$	$+0.05_{-15}^{+14}$	$0.01_{-1}^{+17}$	$(7.4_{-33}^{+42}) \times 10^{-3}$
	1498.8		$2_2^+$	0.72(18)		$+0.294_{-37}^{+31}$	$0.57_{-32}^{+50}$	$(3.1_{-14}^{+18}) \times 10^{-2}$
	2115.1		$2_1^+$	0.228(57)		$+0.394_{-86}^{+96}$	$0.055_{-35}^{+69}$	$(3.3_{-16}^{+22}) \times 10^{-3}$
						$+5.7_{-20}^{+49}$	$0.40_{-18}^{+24}$	$(1.1_{-9}^{+30}) \times 10^{-4}$
2647.0	737.5	(4) <sup>+</sup>	$2_4^+$	0.047(14)	$500_{-160}^{+410}$	$(E2)$	$12_{-7}^{+11}$	
	1089.4		$3_1^+$	0.169(18)			$6.0_{-60}^{+37}$	
	1417.7		$4_1^+$	0.704(32)			$6.8_{-68}^{+36}$	
	2135.4		$2_1^+$	0.080(16)		$(E2)$	$0.099_{-86}^{+75}$	
2699.7	302.1	6 <sub>1</sub> <sup>-</sup>	$5_1^-$	0.704(43)				
	393.5		$4_1^-$	<0.296				
2705.2	998.9	1 <sup>+</sup>	$0_3^+$	0.065(7)	$145_{-17}^{+20}$	$M1$		$(2.56_{-55}^{+65}) \times 10^{-2}$
	1571.3		$0_2^+$	0.018(4)		$M1$		$(1.82_{-58}^{+70}) \times 10^{-3}$
	1577.1		$2_2^+$	0.144(29)			$2.8_{-28}^{+10}$	
	2193.3		$2_1^+$	0.508(26)			$1.9_{-19}^{+4}$	
	2705.3		$0_1^+$	0.265(29)		$M1$		$(5.3_{-11}^{+14}) \times 10^{-3}$
2713.9	1156.2	3 <sup>+</sup>	$3_1^+$	0.421(27)	$400_{-120}^{+270}$		$14_{-14}^{+7}$	
	1484.6		$4_1^+$	0.208(17)			$2.0_{-20}^{+10}$	
	1585.8		$2_2^+$	0.299(32)			$2.0_{-20}^{+12}$	
	2202.0		$2_1^+$	0.071(15)			$0.094_{-94}^{+67}$	
2737.3	659.7	(4) <sup>+</sup>	$4_3^+$	0.51(12)				
	1179.5		$3_1^+$	0.270(63)				
	1508.0		$4_1^+$	0.219(34)				
2741.4	2741.4	1,2 <sup>+</sup>	$0_1^+$	1.000				
2747.7	247.7	3	$3^-$	0.162(17)	$500_{-200}^{+1800}$			
	1518.5		$4_1^+$	0.158(17)			$1.1_{-11}^{+12}$	
	2235.8		$2_1^+$	0.681(44)			$0.71(71)$	
2752.6	668.1	(5)	$3_1^-$	0.058(18)				
	674.9		$4_3^+$	0.057(18)				
	1523.4		$4_1^+$	0.89(12)				

TABLE II. (*Continued.*)

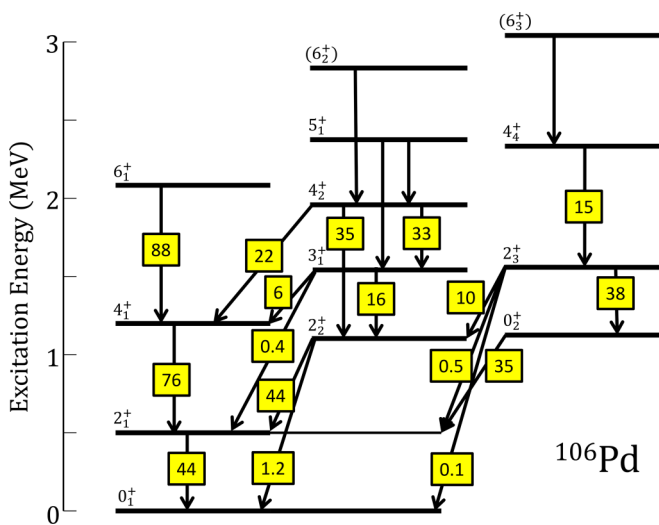
$E_{\text{level}}$ (keV)	$E_{\gamma}$ (keV)	$J_i^{\pi}$	$J_f^{\pi}$	B. R.	$\tau$ (fs)	Multipolarity or $\delta$	$B(E2)$ (W.u.)	$B(E1)/B(M1)$ (W.u.)/( $\mu_N^2$ )
2757.1	391.0 <sup>g</sup>	$5^+_{\text{g}}$	$5^+_1$	0.041(2) <sup>g</sup>				
	406.2		$4^+_5$	0.148(5) <sup>g</sup>		-3.2(2) <sup>a</sup>		
	450.9		$4^-_1$	0.310(10) <sup>g</sup>				
	474.1 <sup>g</sup>		$4^+_4$	0.010(1) <sup>g</sup>		-4.0 <sup>+9</sup> <sub>-6</sub> <sup>a</sup>		
	680.2 <sup>g</sup>		$4^+_3$	0.017(1) <sup>g</sup>				
	824.6		$4^+_2$	0.170(6) <sup>g</sup>		-6.5(6) <sup>a</sup>		
	1199.4 <sup>g</sup>		$3^+_1$	0.124(6) <sup>g</sup>				
	1527.8		$4^+_1$	0.180(15) <sup>g</sup>		-2.46(9) <sup>a</sup>		
2776.0	1213.5	(3,4)	$2^+_3$	0.064(32)	$290^{+330}_{-110}$			
	1217.9		$3^+_1$	0.405(34)				
	1546.7		$4^+_1$	0.136(29)				
	1647.8		$2^+_2$	0.322(69)				
	2264.1		$2^+_1$	0.073(16)				
2783.9	2272.0	2,3	$2^+_1$	1.000	$81^{+7}_{-6}$			
2812.3	734.8	(6 <sup>+</sup> )	$4^+_3$	0.161(51)		(E2)		
	879.8		$4^+_2$	0.237(52)		(E2)		
	1583.0		$4^+_1$	0.602(81)		(E2)		
2820.5	1258.2	2 <sup>+</sup>	$2^+_3$	0.063(19)	$290^{+120}_{-70}$	$+1.4^{+64}_{-58}$	$1.2^{+13}_{-9}$	$2.1^{+42}_{-15}$
						$+0.22^{+31}_{-17}$	$0.08^{+61}_{-8}$	$(5.9^{+46}_{-35}) \times 10^{-3}$
	1692.4		$2^+_2$	0.095(29)		-0.18(10)	$0.02^{+11}_{-2}$	$(3.7^{+28}_{-20}) \times 10^{-3}$
	2308.6		$2^+_1$	0.550(40)		$+4^{+12}_{-2}$	$0.61^{+49}_{-34}$	$(2.1^{+82}_{-20}) \times 10^{-4}$
						$+2.36^{+42}_{-40}$	$0.67^{+31}_{-26}$	$(1.3^{+12}_{-7}) \times 10^{-3}$
	2820.5		$0^+_1$	0.292(33)		E2	$0.153^{+70}_{-57}$	
2828.4	1266.1	(0 <sup>+</sup> )	$2^+_3$	0.153(31)	$300^{+180}_{-90}$	(E2)	$4.3^{+30}_{-22}$	
	2316.6		$2^+_1$	0.847(42)		(E2)	$1.16^{+55}_{-47}$	
2846.2	1283.9		$2^+_3$	0.077(16)	$300^{+150}_{-80}$			
	1616.9		$4^+_1$	0.923(89)				
2850.8	918.4	3	$4^+_3$	0.081(16)	$170^{+37}_{-27}$			
	941.3		$2^+_4$	0.125(19)				
	1621.5		$4^+_1$	0.662(34)				
	1722.6		$2^+_2$	0.132(27)				
2860.3	775.8		$3^-_1$	1.000				
2860.9	1302.9	(5 <sup>+</sup> )	$3^+_1$	0.65(12)		(E2)		
	1632.3		$4^+_1$	0.352(82)				
2875.7	1646.4		$4^+_1$	1.000				
2878.0	1315.8		$2^+_3$	0.107(23)	$800^{+6400}_{-400}$			
	2366.1		$2^+_1$	0.893(86)				
2878.4	1320.6		$3^+_1$	0.093(13)	$380^{+370}_{-130}$			
	1649.1		$4^+_1$	0.91(12)				
2886.2	1758.1	(3)	$2^+_2$	0.620(54)	$323^{+99}_{-63}$			
	2374.4		$2^+_1$	0.380(33)				
2897.5	591.3	4,5 <sup>-</sup>	$4^-_1$	0.255(66)	$360^{+330}_{-120}$			
	813.7		$3^-_1$	0.156(26)				
	1668.1		$4^+_1$	0.589(45)				

TABLE II. (*Continued.*)

$E_{\text{level}}$ (keV)	$E_{\gamma}$ (keV)	$J_i^{\pi}$	$J_f^{\pi}$	B. R.	$\tau$ (fs)	Multipolarity or $\delta$	$B(E2)$ (W.u.)	$B(E1)/B(M1)$ (W.u.)/( $\mu_N^2$ )	
2902.5	1774.3	1,2 <sup>+</sup>	2 <sub>2</sub> <sup>+</sup>	0.158(25) <sup>a</sup>	$87_{-7}^{+8}$				
	2390.6		2 <sub>1</sub> <sup>+</sup>	0.833(32) <sup>a</sup>					
	2902.5		0 <sub>1</sub> <sup>+</sup>	0.008(3) <sup>a</sup>					
2907.5	1678.2		4 <sub>1</sub> <sup>+</sup>	1.000	>270				
2908.7	824.3		3 <sub>1</sub> <sup>-</sup>	0.133(27)	$390_{-90}^{+180}$				
	1346.1		3 <sub>1</sub> <sup>+</sup>	0.074(22)					
	2396.7		2 <sub>1</sub> <sup>+</sup>	0.794(58)					
2918.0	1355.7	2 <sup>+</sup>	2 <sub>3</sub> <sup>+</sup>	0.034(10)	$109_{-11}^{+12}$			$(2.87_{-54}^{+62}) \times 10^{-2}$	
	1360.2		3 <sub>1</sub> <sup>+</sup>	0.143(23)					
	2406.1		2 <sub>1</sub> <sup>+</sup>	0.767(70)					
	2918.2		0 <sub>1</sub> <sup>+</sup>	0.056(9)		<i>E2</i>	0.067 <sup>+19</sup> <sub>-16</sub>		
2935.5	1706.0	(3)	4 <sub>1</sub> <sup>+</sup>	0.130(21)	$99_{-8}^{+9}$				
	1807.3		2 <sub>2</sub> <sup>+</sup>	0.237(38)					
	2424.1		2 <sub>1</sub> <sup>+</sup>	0.633(45)					
2968.5	2456.7		2 <sub>1</sub> <sup>+</sup>	1.000					
2970.7	2458.9		2 <sub>1</sub> <sup>+</sup>	1.000					
2976.7	476.9		3 <sup>-</sup>	0.265(92)	$127_{-31}^{+54}$				
	892.2		3 <sub>1</sub> <sup>-</sup>	0.74(19)					
3022.0	1792.7		4 <sub>1</sub> <sup>+</sup>	1.000	$95_{-13}^{+16}$				
3037.3	1909.2	1	2 <sub>2</sub> <sup>+</sup>	0.190(97)	$35_{-3}^{+4}$				
	3037.3		0 <sub>1</sub> <sup>+</sup>	0.810(93)					
	758.4	(6 <sup>+</sup> )	4 <sub>4</sub> <sup>+</sup>	0.171(35)			<i>(E2)</i>		
3041.6	1812.6		4 <sub>1</sub> <sup>+</sup>	0.829(61)			<i>(E2)</i>		
	1920.5	(1)	0 <sub>2</sub> <sup>+</sup>	0.097(25)	$92_{-18}^{+25}$				
	1926.3		2 <sub>2</sub> <sup>+</sup>	0.088(45)					
3054.4	2542.6		2 <sub>1</sub> <sup>+</sup>	0.734(74)					
	3054.4		0 <sub>1</sub> <sup>+</sup>	0.081(10)					
	1828.4	(3)	4 <sub>1</sub> <sup>+</sup>	0.596(62)	$190_{-42}^{+69}$				
3057.7	1929.6		2 <sub>2</sub> <sup>+</sup>	0.198(62)					
	2545.8		2 <sub>1</sub> <sup>+</sup>	0.206(64)					
	1939.3		2 <sub>2</sub> <sup>+</sup>	0.397(73)	$210_{-70}^{+190}$				
3067.4	2555.5		2 <sub>1</sub> <sup>+</sup>	0.60(11)					
	2559.2		2 <sub>1</sub> <sup>+</sup>	1.000					
	1525.6	(3)	3 <sub>1</sub> <sup>+</sup>	0.40(11)	$240_{-60}^{+120}$				
3083.3	1955.2		2 <sub>2</sub> <sup>+</sup>	0.064(14)					
	2571.5		2 <sub>1</sub> <sup>+</sup>	0.538(62)					
	1868.2		4 <sub>1</sub> <sup>+</sup>	1.000					
3110.8	2599.0	1,2 <sup>+</sup>	2 <sub>1</sub> <sup>+</sup>	0.72(14)					
	3110.9		0 <sub>1</sub> <sup>+</sup>	0.277(53)					
3121.3	2609.4		2 <sub>1</sub> <sup>+</sup>	1.000	$180_{-60}^{+130}$				
3161.1	1076.5	(2,3)	3 <sub>1</sub> <sup>-</sup>	0.224(29)	$74_{-23}^{+43}$				
	2649.3		2 <sub>1</sub> <sup>+</sup>	0.78(10)					

TABLE II. (*Continued.*)

$E_{\text{level}}$ (keV)	$E_{\gamma}$ (keV)	$J_i^{\pi}$	$J_f^{\pi}$	B. R.	$\tau$ (fs)	Multipolarity or $\delta$	$B(E2)$ (W.u.)	$B(E1)/B(M1)$ (W.u.)/( $\mu_N^2$ )
3166.3	2032.4	1	$0_1^+$	0.300(56)	$135^{+70}_{-38}$	<i>M1 or E1</i>		
	2654.4		$2_1^+$	0.32(10)				
	3166.3		$0_1^+$	0.377(49)				
3173.7	2045.4		$2_2^+$	0.54(15)	$320^{+240}_{-100}$	<i>M1 or E1</i>		
	2662.3		$2_1^+$	0.465(81)				
3215.0	1652.7		$2_3^+$	1.000	$290^{+350}_{-110}$			
3221.5	2093.4		$2_2^+$	0.089(20) <sup>b</sup>	$160^{+170}_{-60}$			
	2709.6		$2_1^+$	0.911(38) <sup>b</sup>				
	3249.6	1,2 <sup>+</sup>	$0_1^+$	1.000	28(4)			
3250.5	2738.6		$2_1^+$	1.000	$43^{+21}_{-13}$			
3272.9	3272.9	1,2 <sup>+</sup>	$0_1^+$	1.000	12(3)			
3274.4	2762.5		$2_1^+$	1.000				
3300.2	1737.9	1,2 <sup>+</sup>	$2_3^+$	0.126(22)	$103^{+36}_{-23}$			
	2172.1		$2_2^+$	0.467(83)				
	2788.4		$2_1^+$	0.160(50)				
	3300.4		$0_1^+$	0.247(44)				
3321.4	2809.5		$2_1^+$	1.000				

<sup>a</sup>From Ref. [20].<sup>b</sup>Calculated from the  $B(E2)$  for the  $3_1^+ \rightarrow 2_2^+$  from Ref. [11].<sup>c</sup>Calculated assuming pure  $E2$  multipolarity.<sup>d</sup>Calculated from the  $B(E2)$  for the  $2_3^+ \rightarrow 0_2^+$  from Ref. [8].<sup>e</sup>From Ref. [21].<sup>f</sup>The lifetime and angular distribution for the 1988.3 keV  $\gamma$  ray do not agree with those for the other branches from the 2499.9 keV level. However, the 1988.0 keV  $\gamma$  ray is seen in coincidence with the 476.9 keV  $\gamma$  ray from the 2976.7 keV level, indicating that it is a doublet.<sup>g</sup>From Ref. [22].<sup>h</sup>From Ref. [23].FIG. 5. Levels, spins and parities, and  $E2$  transition probabilities in W.u. (given in boxes) in  $^{106}\text{Pd}$ . See Table II for more detailed information.

Our leading conclusion is that, contrary to the implications of these calculations, “mixed-symmetry” collectivity does not play a significant role at low energy in  $^{106}\text{Pd}$ . Indeed, the mixed-symmetry strength in  $^{106}\text{Pd}$  has been observed above 3 MeV [31].

### C. Band structure in $^{106}\text{Pd}$

In the study of  $E0$  transitions in  $^{106}\text{Pd}$  [10], large  $\rho^2(E0)$  values provided evidence for shape coexistence, extending the observation of such structures to the  $N = 60$  isotones and leading to the determination of  $E0$  strength between levels with  $K = 2$ . ( $K$  is not a good quantum number in nuclei with modest deformation, but it serves as a convenient label.) Low-lying  $K = 0$  and  $K = 2$  bands were identified and are extended in the present work. The lowest-lying of these bands are shown in Fig. 5.

The ground-state band has been characterized in Coulomb excitation [8] and in-beam studies with heavy ions [21,32], but only the lowest members of the band are populated in the INS studies. The character of the  $K = 2$  band has become

TABLE III. Comparison of  $B(E2)s$  in W.u. in  $^{106}\text{Pd}$  with predictions of various models.

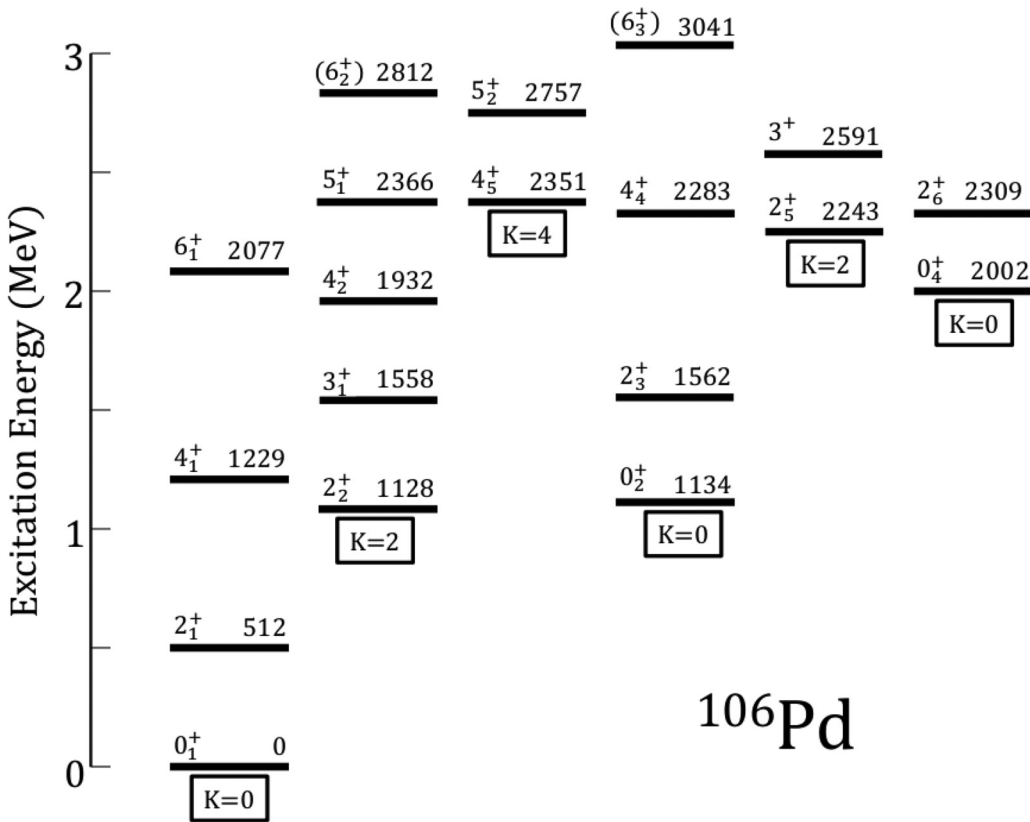
$B(E2)$ sum	Experiment	Vibrational	Gamma-soft rotor	Triaxial rotor	IBM2
$\Sigma 2_i^+ \rightarrow 0_2^+$	$46_{-12}^{+14}$	62	0	0	
$\Sigma 2_i^+ \rightarrow 2_2^+$	$20_{-11}^{+6}$	25.3	0	0	
$\Sigma 4_i^+ \rightarrow 2_2^+$	$35_{-6}^{+8}$	69.2	39	17	40
$\Sigma 3_i^+ \rightarrow 2_2^+$	18(4)	94.8	53	79	53
$\Sigma 2_i^+ \rightarrow 4_1^+$	$16_{-5}^{+6}$	45.6	0	0	
$\Sigma 4_i^+ \rightarrow 4_1^+$	$23_{-5}^{+6}$	63.3	35	12	28
$\Sigma 3_i^+ \rightarrow 4_1^+$	$8_{-7}^{+2}$	38.1	21	41	17

clearer with the identification of additional band members and crossover transitions, and the pattern of interband  $E0$  strength [10] indicates shape coexistence between the lowest  $K = 0$  bands.

Additional  $K = 0, 2$ , and 4 bands are suggested in Fig. 6. Not shown in this figure are  $0^+$  states at 1706, 2278, and 2624 keV, which are likely band heads. Only in the case of the 1706 keV  $0^+$  state has a tentative  $2^+$  member of the band been identified at 1910 keV [10]. Of the positive-parity states below 2.4 MeV, only the  $4^+$  state at 2078 keV could not be placed in a band. This state may be a hexadecapole excitation corresponding to those seen [33] in the heavier stable Pd nuclei near this excitation energy. It was likely obscured by the strong excitation of the nearby lowest negative-parity state,  $3^-$  at 2084 keV, in inelastic proton and deuteron scattering measurements [33].

#### D. Negative-parity states

In addition to the previously mentioned 2084 keV  $3^-$  state, the octupole phonon, several additional negative-parity states are observed above 2 MeV in excitation energy. In other nuclei in this mass region, the coupling between the quadrupole and octupole phonon states ( $2_1^+ \otimes 3_1^-$ ) leads to a quintuplet of negative-parity states with spins between  $1^-$  and  $5^-$ , lying near the summed energy of the phonons [ $E(2_1^+) + E(3_1^-)$ ]. These states are expected to decay by enhanced  $E2$  and  $E3$  transitions, which correspond to the destruction of the respective phonons. While negative-parity states in the expected energy region have been assigned, i.e., 2306 keV ( $4^-$ ), 2397 ( $5^-$ ), 2401 ( $2^-, 3^-$ ), 2485 ( $1^{(-)}$ ), and 2500 ( $3^-$ ), and most exhibit decays to the 2084 keV  $3^-$  state, the decays of none of these states are remarkably enhanced; thus it is difficult to comment on their underlying nuclear structure.

FIG. 6. Levels in  $^{106}\text{Pd}$  shown as  $K = 0, 2$ , and 4 bands.

#### IV. CONCLUSIONS

In summary, inelastic neutron scattering has been used to determine level lifetimes, spins, branching ratios, and multipole mixing ratios for transitions from all known positive-parity states in  $^{106}\text{Pd}$  up to  $\approx 2.4$  MeV. The  $B(E2)$  values for transitions from these states have been determined and provide an unprecedented view of collectivity in this nucleus. To further test this view, it will be necessary to observe low-energy  $\gamma$  rays between high-lying levels, i.e., in-band rotational transitions. This is not possible with  $(n,n'\gamma)$  measurements because the low-energy  $\gamma$  rays are absorbed in the necessarily

massive scattering samples, but  $\beta$ -decay studies are well suited [34] to this task and should be pursued.

#### ACKNOWLEDGMENTS

The authors sincerely thank H.E. Baber for his contributions in maintaining the Van de Graaff accelerator. This material is based upon work supported by the US National Science Foundation under Grant No. PHY-1606890. The isotope used in this research was supplied by the United States Department of Energy Office of Science by the Isotope Program in the Office of Nuclear Physics.

- 
- [1] A. Bohr, Mat. Fys. Medd. Dann. Vid. Selsk. **26**, 1 (1952).
  - [2] P. E. Garrett, K. L. Green, and J. L. Wood, *Phys. Rev. C* **78**, 044307 (2008).
  - [3] K. L. Green, P. E. Garrett, R. A. E. Austin, G. C. Ball, D. S. Bandyopadhyay, S. Colosimo, D. Cross, G. A. Demand, G. F. Grinyer, G. Hackman, W. D. Kulp, K. G. Leach, A. C. Morton, C. J. Pearson, A. A. Phillips, M. A. Schumaker, C. E. Svensson, J. Wong, J. L. Wood, and S. W. Yates, *Phys. Rev. C* **80**, 032502 (2009).
  - [4] P. E. Garrett and J. L. Wood, *J. Phys. G* **37**, 064028 (2010).
  - [5] P. E. Garrett, K. L. Green, H. Lehmann, J. Jolie, C. A. McGrath, M. Yeh, and S. W. Yates, *Phys. Rev. C* **75**, 054310 (2007).
  - [6] D. Bandyopadhyay, S. R. Lesher, C. Fransen, N. Boukharouba, P. E. Garrett, K. L. Green, M. T. McEllistrem, and S. W. Yates, *Phys. Rev. C* **76**, 054308 (2007).
  - [7] M. Kadi, N. Warr, P. E. Garrett, J. Jolie, and S. W. Yates, *Phys. Rev. C* **68**, 031306 (2003).
  - [8] L. E. Svensson, C. Fahlander, L. Hasselgren, A. Bäcklin, L. Westerberg, D. Cline, T. Czosnyka, C. Y. Wu, R. M. Diamond, and H. Kluge, *Nucl. Phys. A* **584**, 547 (1995).
  - [9] G. Gürdal, G. J. Kumbartzki, N. Benczer-Koller, Y. Y. Sharon, L. Zamick, S. J. Q. Robinson, T. Ahn, R. Casperson, A. Heinz, G. Ilie, J. Qian, V. Werner, E. Williams, R. Winkler, and D. McCarthey, *Phys. Rev. C* **82**, 064301 (2010).
  - [10] E. E. Peters, F. M. Prados-Estévez, A. Chakraborty, M. G. Mynk, D. Bandyopadhyay, S. N. Choudry, B. P. Crider, P. E. Garrett, S. F. Hicks, A. Kumar, S. R. Lesher, C. J. McKay, J. N. Orce, M. Scheck, J. R. Vanhoy, J. L. Wood, and S. W. Yates, *Eur. Phys. J. A* **52**, 96 (2016).
  - [11] L. E. Svensson, Ph.D. thesis, University of Uppsala, 1989 (unpublished).
  - [12] P. E. Garrett, N. Warr, and S. W. Yates, *J. Res. Natl. Inst. Stand. Technol.* **105**, 141 (2000).
  - [13] E. Sheldon and V. C. Rogers, *Comput. Phys. Commun.* **6**, 99 (1973).
  - [14] P. A. Moldauer, *Phys. Rev. C* **14**, 764 (1976).
  - [15] T. Belgya, G. Molnár, and S. W. Yates, *Nucl. Phys. A* **607**, 43 (1996).
  - [16] K. B. Winterbon, *Nucl. Phys. A* **246**, 293 (1975).
  - [17] A. Fitzler, Tv User Manual, Institute for Nuclear Physics, University of Cologne (2000).
  - [18] C. A. McGrath, P. E. Garrett, M. F. Villani, and S. W. Yates, *Nucl. Instrum. Methods Phys. Res., Sect. A* **421**, 458 (1999).
  - [19] D. C. Radford, *Nucl. Instrum. Methods Phys. Res., Sect. A* **361**, 297 (1995).
  - [20] D. De Frenne and A. Negret, *Nucl. Data Sheets* **109**, 943 (2008).
  - [21] J. A. Grau, L. E. Samuelson, F. A. Rickey, P. C. Simms, and G. J. Smith, *Phys. Rev. C* **14**, 2297 (1976).
  - [22] H. Inoue, *J. Phys. Soc. Jpn.* **35**, 957 (1973).
  - [23] R. Kaur, A. K. Sharma, S. S. Sooch, N. Singh, and P. N. Trehan, *J. Phys. Soc. Jpn.* **51**, 23 (1982).
  - [24] D. De Frenne and E. Jacobs, *Nucl. Data Sheets* **72**, 1 (1994).
  - [25] P. J. Tivin, B. Singh, and H. W. Taylor, *J. Phys. G: Nucl. Phys.* **3**, 1267 (1977).
  - [26] E. A. Coello Pérez and T. Papenbrock, *Phys. Rev. C* **92**, 064309 (2015).
  - [27] K.-H. Kim, A. Gelberg, T. Mizusaki, T. Otsuka, and P. von Brentano, *Nucl. Phys. A* **604**, 163 (1996).
  - [28] M. Büyükkata, P. Van Isacker, and İ. Uluer, *J. Phys. G* **37**, 105102 (2010).
  - [29] P. Van Isacker and G. Puddu, *Nucl. Phys. A* **348**, 125 (1980).
  - [30] A. Giannatiempo, A. Nannini, and P. Sona, *Phys. Rev. C* **58**, 3316 (1998).
  - [31] R. De Leo, L. Lagamba, N. Blasi, S. Micheletti, M. Pignanelli, M. Fujiwara, K. Hosono, I. Katayama, N. Matsuoka, S. Morinobu, T. Noro, S. Matsuki, H. Okamura, J. M. Schippers, S. Y. Van Der Werf, and M. Harakeh, *Phys. Lett. B* **226**, 5 (1989).
  - [32] C. Y. He, B. B. Yu, L. H. Zhu, X. G. Wu, Y. Zheng, B. Zhang, S. H. Yao, L. L. Wang, G. S. Li, X. Hao, Y. Shi, C. Xu, F. R. Xu, J. G. Wang, L. Gu, and M. Zhang, *Phys. Rev. C* **86**, 047302 (2012).
  - [33] M. Pignanelli, N. Blasi, S. Micheletti, R. De Leo, L. LaGamba, R. Perrino, J. A. Bordewijk, M. A. Hofstee, J. M. Schippers, S. Y. van der Werf, J. Wesseling, and M. N. Harakeh, *Nucl. Phys. A* **540**, 27 (1992).
  - [34] A. Chakraborty, E. E. Peters, B. P. Crider, C. Andreoiu, P. C. Bender, D. S. Cross, G. A. Demand, A. B. Garnsworthy, P. E. Garrett, G. Hackman, B. Hadinia, S. Ketelhut, A. Kumar, K. G. Leach, M. T. McEllistrem, J. Pore, F. M. Prados-Estévez, E. T. Rand, B. Singh, E. R. Tardiff, Z.-M. Wang, J. L. Wood, and S. W. Yates, *Phys. Rev. Lett.* **110**, 022504 (2013).